A sea surface temperature reconstruction for the southern Indian Ocean trade wind belt from corals in Rodrigues Island (19° S, 63° E)

Biogeosciences Discuss., doi:10.5194/bg-2016-69, 2016
Manuscript under review for journal Biogeosciences
Published: 3 March 2016

Biogeosciences Discussions
Open Access
EGU

A sea surface temperature reconstruction for the southern Indian Ocean trade wind belt from corals in Rodrigues Island (19°S, 63°E)

J. Zinke[1,2,3], L. Reuning[4], M. Pfeiffer[4], J. Wassenburg[5], E. Hardman[6], R. Jhangeer-Khan[6], Davies, G. R.[7], C.K.C. Ng[8], and D. Kroon[9]

[1]Department of Environment and Agriculture, Curtin University of Technology, Kent Street, Bentley, WA6102, Australia

[2]Australian Institute of Marine Science, Nedlands, WA 6009, Australia

[3]School of Geography, Archaeology and Environmental Studies, University of Witwatersrand, Johannesburg, South Africa.

[4]Institute for Geology, RWTH Aachen, Wuellnerstrasse2, 52056 Aachen, Germany

[5]Institute for Geosciences, Johannes-Gutenberg-University Mainz, Johann-Joachim-Becher-Weg 21, D-55128 Mainz

[6]SHOALS Rodrigues, Rodrigues, Mauritius

[7]Department of Petrology, VU University Amsterdam, De Boelelaan 1085, 1081 HV Amsterdam, Netherlands

[8]Department of Medical Radiation Sciences, Curtin University of Technology, Kent Street, Bentley, WA6102, Australia

[9]University of Edinburgh, School of GeoSciences, The King's Buildings, West Mains Road, Edinburgh EH9 3JW, UK.

Correspondence to: Jens Zinke, jens.zinke@gmail.com

Biogeosciences Discuss., doi:10.5194/bg-2016-69, 2016
Manuscript under review for journal Biogeosciences
Published: 3 March 2016

Abstract

The western Indian Ocean has been warming rapidly over the past decades and this has adversely impacted the Asian Monsoon circulation. It is therefore of paramount importance to improve our understanding of links between Indian Ocean Sea Surface Temperature (SST) variability, climate change, and sustainability of reef ecosystems. Here we present two monthly-resolved coral Sr/Ca records (Totor, Cabri) from Rodrigues Island (63°E, 19°S) in the south-central Indian Ocean trade wind belt, and reconstruct SST based on the linear relationship with the Sr/Ca proxy. The records extend to 1781 and 1945, respectively. We assess the reproducibility of the Sr/Ca records, and potential biases in our reconstruction associated with the orientation of corallites. We quantify long-term SST trends and identify interannual relationships with the El Niño-Southern Oscillation (ENSO) and the Pacific Decadal Oscillation (PDO). We conclude that careful screening for diagenesis and orientation of corallites is of paramount importance to assess the quality of Sr/Ca-based SST reconstructions. Our proxy records provide a reliable SST reconstruction between 1945 and 2006. We identify strong teleconnections with the ENSO/PDO over the past 60 years, eg. warming of SST during El Niño or positive PDO. We suggest that additional records from Rodrigues Island can provide excellent records of SST variations in the southern Indian Ocean trade wind belt and teleconnections with the ENSO/PDO on longer time scales.

1 Introduction

The Indian Ocean has been warming steadily over the past century with the western portion of the basin having experienced an increase in SST of up to 1.2°C over the past

Biogeosciences Discuss., doi:10.5194/bg-2016-69, 2016
Manuscript under review for journal Biogeosciences
Published: 3 March 2016

60 years (Koll Roxy et al., 2014). The Indian Ocean has also taken up a large amount of heat in its interior during the recent 15 years when global SST increased at a smaller rate as compared to previous decades (Lee et al., 2015). The strong Indian Ocean warming over the past century is thought to have contributed to a decreasing land-sea thermal contrast with the Indian subcontinent affecting monsoon rainfall and might have played a major role for the decrease in East African rainfall between March to May in recent decades (Funk et al., 2008; Koll Roxy et al., 2015). The western Indian Ocean warming has also been shown to follow closely anthropogenic radiative forcing over the past century (Funk et al., 2008; Alory et al., 2009; Koll Roxy et al., 2015). Furthermore, the western Indian Ocean warmed significantly during past El Niño events with the 1997/98 event having caused widespread coral bleaching and mortality. It is therefore of paramount importance to improve our understanding of links between Indian Ocean SST variability, global climate change, and sustainability of reef ecosystems. Yet, long-term observational records of Indian Ocean SST are sparse and are thought to be only reliable after the 1960's (Tokinaga et al., 2012). To overcome the limitations of the short observational record, paleoclimate records of past SSTs can be generated to provide insight into long-term SST changes and interannual to decadal variability.

Paleoclimate reconstructions of SST from massive corals have provided invaluable records for past SST trends and interannual to decadal variability in the western Indian Ocean (Charles et al., 1997; Cole et al., 2000; Cobb et al., 2001; Pfeiffer et al., 2004, 2009; Pfeiffer & Dullo, 2006; Nakamura et al., 2009; Crueger et al., 2009; Grove et al., 2013; Zinke et al. 2008, 2009, 2014). Massive corals, such as *Porites* spp., can grow for centuries and grow at a rate between 0.5 and 2 cm yr^{-1}. Therefore, down-

Biogeosciences Discuss., doi:10.5194/bg-2016-69, 2016
Manuscript under review for journal Biogeosciences
Published: 3 March 2016

core sampling of massive corals yields an in situ SST time series of monthly resolution. As the coral precipitates its skeleton, trace elements and stable isotopes are incorporated at different concentrations, relative to Ca, in relation to changing SSTs (Felis and Pätzold, 2003). Both, the Sr/Ca ratio and $\delta^{18}O$ composition of the coral aragonite were shown to be reliable paleo-thermometers, whereby a negative relationship exists with SST (Alibert and McCulloch, 1997; Pfeiffer & Dullo, 2006; DeLong et al., 2012). A compilation of Sr/Ca-SST calibrations for Porites *spp.* revealed a mean Sr/Ca relationship with SST of -0.061mmol/mol/1°C SST increase (Corrège, 2006). Since Sr has a long oceanic residence time, skeletal Sr/Ca is assumed to mainly reflect SST variability. The quality and accuracy of paleo-thermometers strongly depends on optimal sampling of the major growth axes (De Long et al., 2012). Furthermore, diagenetic alterations of coral aragonite can lead to errors in SST reconstructions and need to be excluded by specific analysis (McGregor and Gagan, 2003; McGregor and Abram, 2008; Sayani et al., 2011; Smodej et al., 2015).

Currently, none of the coral proxy records from the western Indian Ocean cover the south-central Indian Ocean basin in the heart of the trade wind system. Furthermore, all proxy records of interest for the trade wind belt are based on oxygen isotopes with the exception of two Sr/Ca ratio records covering 1952 to 2008 from St. Marie Island off East Madagascar (Grove et al., 2013). The latter provided mixed results with discrepancies in terms of the long-term SST trend estimates due to confounding effects of coral calcification in at least one of the cores (Grove et al., 2013). A coral oxygen isotope record from Reunion Island (21°S, 55°E; Mascarene Islands) located approximately 230km to the southwest of Mauritius spans the period 1832 to 1994 and is the longest for

Biogeosciences Discuss., doi:10.5194/bg-2016-69, 2016
Manuscript under review for journal Biogeosciences
Published: 3 March 2016

95 the subtropical region off East Madagascar (Pfeiffer et al., 2004). Pfeiffer et al. (2004)
96 showed evidence that the La Reunion coral dominantly recorded past variations in the
97 salinity anomalies associated with transport changes of the South Equatorial Current. The
98 proxy record showed decadal anomalies that were opposite to those of SST. Crueger et al.
99 (2009) showed close linkages of the salinity, SLP and SST signal associated with the
100 Pacific Decadal Oscillation (Mantua et al., 1997) in coral records from Reunion and Ifaty
101 (SW Madagascar), respectively. Two coral oxygen isotope records from the Seychelles
102 located in the tropical western Indian Ocean (5°S, 54°E) were interpreted as an excellent
103 record of past Southwest Monsoon SST changes and showed strong correlations with air
104 temperatures over India between 1847 to 1994 (Charles et al., 1997; Pfeiffer & Dullo,
105 2006). Both, the Reunion and Seychelles records showed strong correlations with the El
106 Nino-Southern Oscillation on interannual and decadal time scales (Pfeiffer & Dullo,
107 2006).

108 Here, we aim to reconstruct past SSTs from Sr/Ca ratios in two coral cores
109 obtained from Rodrigues Island (19°S, 63°E) located 500 km to the North-East of
110 Mauritius within the trade wind belt of the south-central Indian Ocean. We assess the
111 reproducibility of the Sr/Ca proxy from two different locations, their long-term trends and
112 interannual variability related to the El Nino-Southern Oscillation.
113

114 **2 Regional setting and climate**

115 Rodrigues (63°E, 19°S) is a small volcanic island in the southern Indian Ocean, about
116 619 km east of Mauritius (Fig. 1). It is part of the eastern edge of the Mascarene Plateau
117 that is made up of Lower Tertiary basalts (Mart 1988) that formed by a seaward flow of

Biogeosciences Discuss., doi:10.5194/bg-2016-69, 2016
Manuscript under review for journal Biogeosciences
Published: 3 March 2016

lava, which has been eroded by hydrodynamic forces, and biological and chemical processes (Turner and Klaus, 2005). Rodrigues has a surface area of about 119 km^2, with a maximum altitude of 396 meter above sea level and is surrounded by a nearly continuous fringing reef, which form an almost continuous band measuring approximately 90km in length (Turner and Klaus, 2005; Lynch et al. 2002). The reef encloses a shallow lagoon, which, at 240km^2, is twice the area of the island itself. The maximum tidal range is approximately 1.5m, and since the average water depth in the lagoon is less than 2m, some areas are exposed at low spring tides. The water depth immediately beyond the reef slopes is usually within the range of 10m to 30m. The island has three major channels, one dredged channel for the main harbour at Port Mathurin in the north, and natural channels in the south near Port Sud Est and in the East at St Francois. Several small passes are also found at intervals around the reef (Turner and Klaus, 2005).

The water surrounding Rodrigues is supplied by the South Equatorial Current (SEC) (New et al. 2007) which is a broad east to west current between 10º and 20º S in the Indian Ocean driven by the southeast trade winds (Schott and McCreary, 2001). The southern part of the SEC water flows in several directions, alongside Rodrigues in southwest and southeast direction, and westward to Mauritius (New et al. 2007).

Rodrigues has a relatively dry climate and evaporation exceeds precipitation on the annual mean. Yearly precipitation is ~1000 mm with most precipitation from January to April related to the position of the Inter Tropical Convergent Zone (ITCZ). Between November and March, the Southern Indian Ocean is affected by tropical cyclones, as a result of warm SSTs and a strong convergence between northeast and southeast trades.

Biogeosciences Discuss., doi:10.5194/bg-2016-69, 2016
Manuscript under review for journal Biogeosciences
Published: 3 March 2016

141 Rodrigues experiences two to sixteen cyclones per year, of which 2.5 are extreme: with
142 winds of 280 km/h and waves that reach 100 m inland and 2 m above sea level. They
143 usually last five to ten days (Turner and Klaus, 2005).

144 SST was monitored *in situ* by a CTD 150m offshore from the northern fringing reefs
145 at Totor between 2002 to 2006 (Fig. 2a). Maximum SST are recorded between December
146 to March (28.6 ± 0.5ºC) and minimum SST between July to September (22.4 ± 0.27ºC).
147 Annual mean SST is 25.49 ± 0.24ºC with a seasonal amplitude of 6.22 ± 0.68ºC (Fig. 2a).

148 Air temperatures are recorded by the WMO weather station located at the northern
149 coast of Rodrigues since 1951 and are available at http://climexp.knmi.nl/. The most
150 recent years between 1997 and 2007 have been provided by the Rodrigues
151 Meteorological Office (Fig. 2b). The warmest months are December to March (31.2 ±
152 0.3º), the coldest months are July to September (24.2 ± 0.3º). Yearly average air
153 temperature is 27.49ºC ± 0.31ºC with a yearly amplitude of about 7 ± 0.79ºC.

154

155 **3 Materials and Methods**

156 Two cores were drilled from massive, dome-shaped *Porites* sp. and *Porites lobata*
157 at the northern reef sites Totor (S19º67062; E63º42923) and Cabri (S19°667171,
158 E63°43.4423), respectively (Fig. 1; Table 1). The size of the coral colonies at Totor is
159 ~2.5m and that of Cabri is ~4m in height. Both colonies were healthy and showed no
160 signs of disease or dead surfaces at the time of drilling. The 220cm long core Totor was
161 obtained in August 2005 from the forereef slope of the northern fringing reef facing the
162 open ocean with the top of the colony at 4m water depth. The 180cm long core Cabri was
163 obtained in March 2007 growing in 3m water depth about 1km to the northeast of Totor

Biogeosciences Discuss., doi:10.5194/bg-2016-69, 2016
Manuscript under review for journal Biogeosciences
Published: 3 March 2016

164 from the outer fringing reef. The site Cabri is more exposed to trade winds as compared
165 to Totor which is more sheltered.

166 A commercially available pneumatic drill driven by scuba tanks was used to
167 extract cores along the central growth axis, with a diameter measuring 4 cm. Cores were
168 sectioned into 7 mm thick slabs, rinsed several times with demineralised water, blown
169 with compressed air to remove any surficial particles and dried for more than 24 hours in
170 a laminar flow hood. Growth laminae were visualised by X-radiograph-positive prints,
171 and the growth axis of the coral slab was defined as the line normal to these laminae
172 (Appendix Fig. 7 and 8). Coral densities (g/cm^3) were calculated by analysing digital X-
173 rays using the program CoralXDS and densitometry (Helmle et al., 2011; Carricart-
174 Ganivet et al., 2007), calcification rate ($g/cm^2\ yr^{-1}$) by multiplying density with extension
175 rate. The annual extension rates ($cm\ yr^{-1}$) were calculated by measuring the distance (cm)
176 between density minima using the program CoralXDS. With a diamond coated drill
177 mounted on top of a movable frame, samples were taken every 1 mm parallel to the
178 growth axis, equivalent to approximately monthly resolution.

179 A combination of X-ray images, X-ray diffraction (XRD), light and scanning
180 electron microscopy (SEM) with Energy Dispersive X-Ray Spectrometer (EDS) was used
181 to investigate possible diagenetic alteration from cores Totor and Cabri. All coral slabs
182 from cores Toto and Cabri were initially screened for diagenetic alterations using X-ray
183 images (Figs. A7, A8). Corals that showed an annual density banding without anomalous
184 high or low density patches were selected for further study and considered free from
185 obvious diagenetic alteration. Representative samples were chosen from both cores based
186 on the X-ray images for SEM, thin-section and XRD analysis. Additional samples were

Biogeosciences Discuss., doi:10.5194/bg-2016-69, 2016
Manuscript under review for journal Biogeosciences
Published: 3 March 2016

selected after geochemical analysis targeting intervals with unusually high or low Sr/Ca ratios. The powder-XRD diffractometer at RWTH Aachen University was calibrated to detect and quantify very low calcite contents (detection limit ~ 0.2%) following the method described by Smodej et al. (2015). In addition, the 2D-XRD system Bruker D8 ADVANCE GADDS was used for XRD point-measurements directly on the coral slab with a spatial resolution of ~ 4 mm and a calcite detection limit of ~ 0.2% (Smodej et al., 2015). A 2-dimensional detector allows the simultaneous data collection over a large 2 θ range, which reduces the counting time to 10 min for each sampling spot. The coral is mounted on a motorized XYZ-stage and the position of each sample spot is controlled by an automated laser-video alignment system. Multiple sample points can be predefined and measured automatically. This method was used to test for the presence of secondary calcite along the geochemical sample traces of both corals.

Sr/Ca ratios were measured at the University of Kiel with a simultaneous inductively coupled plasma optical emission spectrometer (ICP-OES, Spectro Ciros CCD SOP; Zinke et al., 2014). Approximately 0.5mg of coral powder are dissolved in 1.00 ml 0.2M HNO_3. Prior to analysis, this digest solution is diluted with 0.2M HNO_3 to a final concentration of approx. 8ppm Ca. An in-house coral powder standard (Mayotte) was prepared in an analogue way and used as consistency standard, being re-analyzed after every six samples. The international reference material JCp-1 (coral powder) was analyzed with every sample batch. All calibration solutions are matrix-matched to 8 ppm Ca. Strontium and Ca are measured at their 407 and 317 nm emission lines. Our intensity ratio calibration strategy combines the techniques described by de Villiers et al. (2002)

Biogeosciences Discuss., doi:10.5194/bg-2016-69, 2016
Manuscript under review for journal Biogeosciences
Published: 3 March 2016

and Schrag (1999). Analytical precision of Sr/Ca determinations as estimated from replicate measurements of unknown samples is 0.15% or 0.01 mmol/mol (1sigma).

The coral core chronologies were developed based on the seasonal cycle of Sr/Ca. We assigned the coldest month (either August or September) to the highest measured Sr/Ca ratio in any given year, according to both *in situ* SST and grid-SST (Extended reconstructed SST; Smith et al., 2008). We then interpolated linearly between these anchor points to obtain age assignments for all other Sr/Ca measurements. In a second step, the Sr/Ca data were interpolated to 12 equidistant points per year to obtain monthly time series using AnalySeries 2.0 (Paillard et al., 1996). This approach creates a non-cumulative time scale error of 1 - 2 month in any given year, due to interannual differences in the exact timing of peak SST. The monthly interpolated Sr/Ca time series were cross-checked with the chronologies from coral XDS to reveal the timing of high and low density banding. High density bands in both corals formed in summer (low Sr/Ca) of any given year.

4 Historical SST data

Historical SST data collected primarily by ships-of-opportunity have been summarised in the comprehensive ocean atmosphere data set (ICOADS) to produce monthly averages on a 2°x2° grid basis (Woodruff et al., 2005). In the grid that includes Rodrigues Island the data are extremely sparse (http://climexp.knmi.nl). We therefore extracted SST from extended reconstructed SST (ERSST version 3b/v4; Smith et al., 2008), also based on ICOADS data, which uses sophisticated statistical methods to reconstruct SST in time of sparse data. From ERSST, we extracted data in the 2°x2° grid centred at 61-63°E, 19-

Biogeosciences Discuss., doi:10.5194/bg-2016-69, 2016
Manuscript under review for journal Biogeosciences
Published: 3 March 2016

21°S (Table A1). Between 2002 and 2006 (*in situ* data coverage) ERSST version 3b shows a yearly average of about 25.57C ± 0.19ºC with a yearly amplitude of 5.14 ± 0.39ºC (Smith et al., 2008). The warmest months are February and March with a SST of 28.29ºC ± 0.4ºC, the coldest months are August and September with a SST of 23.15ºC ± 0.13ºC.

Furthermore, we used Met Office Hadley Centre's sea ice and sea surface temperature (HadISST) data for the grid 62-63°E, 19-20°S (Rayner et al., 2003; Kennedy et al., 2011; Table A1). HadISST temperatures are reconstructed using a two-stage reduced-space optimal interpolation procedure, followed by superposition of quality-improved gridded observations onto the reconstructions to restore local detail. Since January 1982, SST time series for HadISST use the optimal interpolation SST (OISST; 1°x1°), version 2 (Reynolds et al., 2002) that includes continuous time series of satellite-based SST measurements. We also extracted Advanced Very High Resolution Radiometer (AVHRR) SST at 0.25°x0.25° resolution (Reynolds et al., 2007) from 1985 to 2006 which is also used by NOAA's coral reef watch. AVHRR SST for Rodrigues between 2002 and 2006 (*in situ* data coverage) provided from NOAA at 0.25°x0.25° resolution (Reynolds et al., 2007) shows a yearly average of 25.4 ± 0.11ºC with a yearly amplitude of 5.9 ± 0.58ºC. Warmest SSTs are observed between January and March (28.65 ± 0.44ºC) and coolest SST between July to September (22.75 ± 0.21ºC).

SST from the 5°x5° HadSST3, the most sophisticated bias-corrected SST data to date, were downloaded for the region 60-65°E, 15-20°S (Kennedy et al., 2011; Appendix Table 1). Yet, HadSST3 contains data gaps throughout the record due to strict quality control. SST is reported as anomalies relative to the 1961 to 1990 mean climatology.

Biogeosciences Discuss., doi:10.5194/bg-2016-69, 2016
Manuscript under review for journal Biogeosciences
Published: 3 March 2016

In addition, we extracted 5°x5° nigh-time marine air temperature data from HadMAT1 and HadNMAT2 datasets (Kent et al., 2013). HadNMAT2 contains data gaps throughout the record due to strict quality control. Night-time marine surface air temperature is highly correlated with SST but free of the biases introduced by changes in SST measurement techniques (Tokinaga et al., 2012).

5 Results

5.1 Coral growth parameters

The average growth rate of the corals Totor (224 years) and Cabri (130 years) over all years of growth were 9.82±0.19mm y^{-1} and 11.79±0.25mm y^{-1}, respectively (Table 1; Fig. A1). The Cabri core shows a growth disturbance at 1907 that led to partial colony death. This is confirmed by three additional cores taken from this colony at different angles which all showed the mortality event marked by a dead surface pre-dating ~1907. This lower core section is overprinted by diagenesis and it is therefore not suitable for climate studies or to determine density and calcification rates.

Extension rate of the Cabri coral shows no long-term trend, yet shows high interannual and decadal variability (Fig. A1). The same holds for calcification rates. Both extension and calcification show marked interannual oscillation in the recent 10 years. Skeletal density shows multidecadal oscillations with high densities between 1907 and 1935, the early 1940's, between 1958 and 1966 and 1980 and 2006, with lower densities in between (Fig. A1).

The Totor core shows a similar decadal and interannual variability in extension and calcification compared to the Cabri core for the period of overlap between 1877 and

Biogeosciences Discuss., doi:10.5194/bg-2016-69, 2016
Manuscript under review for journal Biogeosciences
Published: 3 March 2016

2005 (Fig. A1). The fit is less optimal between 1877 and 1907 due to the dead surface in Cabri that has obscured density banding. No significant trend is observed in both extension and calcification rates over the entire record length. Skeletal density differs between the two cores. The Totor core shows multi-decadal cycles in density superimposed on a decreasing trend and larger magnitude density anomalies compared to the Cabri core. Between 1960 and 2005 both density profiles agree well in terms of decadal variability, both showed a significant drop since the late 1960's and recovery thereafter. However, the low density period in the Totor core lasted several years longer.

5.2 Seasonality, trends and variability in Sr/Ca and instrumental SST time series

For the period of overlap between both cores (1945 to 2005) there is a between colony offset in mean Sr/Ca of 0.0242 mmol/mol. Both cores show a distinct seasonality in Sr/Ca throughout their record length (Fig. 3). The seasonality in the Totor core (0.283±0.049 mmol/mol) is on average slightly higher compared to the Cabri core (0.238±0.055 mmol/mol), yet both overlap within 1σ.

To eliminate the offset between Sr/Ca time series we calculated Sr/Ca anomalies by subtracting their mean relative to the 1961 to 1990 reference period (Figure 3). We subsequently calculated relative changes in SST based on the established empirical relationship of -0.0607 mmol/mol per 1°C derived from >30 published Sr/Ca calibrations (Corrège, 2006). A composite coral temperature record was then constructed by (1) converting each proxy record to temperature units, (2) calculating the arithmetic mean of the coral records from each site, and (3) averaging the mean records from both sites.

Biogeosciences Discuss., doi:10.5194/bg-2016-69, 2016
Manuscript under review for journal Biogeosciences
Published: 3 March 2016

Between 1945 and 2006 both cores indicate higher Sr/Ca anomalies (a period of cooling) that started in the mid 1950's and lasted until the early 1970's. Both cores show a pronounced trend to more negative Sr/Ca values (warming) starting in the 1970's and reduced seasonality in that period (Fig. 3). After 1984 Sr/Ca in the Cabri core further decreases (warms) while core Sr/Ca in the Totor core has no trend. The detrended Sr/Ca time series indicated that both cores show similar decadal oscillations between 1945 and 2005 (not shown). This highlights that the long-term trend estimates after 1984 need to be viewed with caution.

The Sr/Ca time series in the Totor core extends to 1781. Marked negative Sr/Ca anomalies (warmer) are observed during the first half of the 20th century centered at 1918/19, 1936-41 and in the period 1947-1951 that exceed anomalies in the 1961 to 1990 reference period. Sr/Ca anomalies between 1850 and1900 are higher (cooler) while decadal periods with lower (warmer) Sr/Ca are observed between 1781 and 1850 relative to 1961 to 1990. The long-term trend in Sr/Ca anomalies between 1781 and 2005 converted to SST indicated an overall warming of 0.44°C.

The composite Sr/Ca time series displays interannual and decadal variability throughout the record between 1781 and 2006. The anomaly around 1918/19 is the lowest (warmest) of the entire record length. In general, Sr/Ca anomalies during the 20th century are lower (warmer) than between 1850 and 1900, while anomalies between 1781 and 1850 reach similar levels relative to the period 1961 to 1990 for several decades with short-lived excursions to higher (cooler) anomalies. The long-term trend in Sr/Ca anomalies between 1781 and 2006 converted to SST indicated an overall warming of 0.37°C.

Biogeosciences Discuss., doi:10.5194/bg-2016-69, 2016
Manuscript under review for journal Biogeosciences
Published: 3 March 2016

323

324 **5.3 Calibration/validation of coral Sr/Ca-SST**

325 We calibrated the coral Sr/Ca from both cores with *in situ* SST, ERSSTv.3b and
326 AVHRR SST for the period 2002 to 2006 using the minima and maxima in any given
327 year, as well as monthly values with AVHRR SST for 1981 to 2006 (Fig. 4; Tab. A2).
328 The slopes of the ordinary least squares regressions vary between -0.0384 to -0.0638
329 mmol/mol per 1°C (Tab. A2). The lowest slopes are obtained with *in situ* SST and the
330 highest with ERSSTv.3b (Tab. A2). We reconstructed absolute SST for the period of
331 overlap with *in situ* SST from 2002 to 2006 from both coral cores (Fig. 4). The Sr/Ca-
332 SST in the Totor core shows the best fit with *in situ* SST in terms of the seasonal
333 amplitude. The Sr/Ca-SST in the Cabri core overestimates the winter SST of 2002 and
334 2005, yet agrees well for 2003 and 2004 (Fig. 4). However, taking into account the
335 uncertainties (measurement error, regression error) around absolute SST from Sr/Ca for
336 Cabri and Totor of 1.23°C and 1.05°C (1σ), respectively, the coral data agree with *in situ*
337 SST within the 1σ uncertainty.

338 To eliminate large errors associated with absolute SST reconstructions from coral
339 Sr/Ca we calculated relative changes in SST for the composite coral temperature record
340 relative to the 1961 to 1990 mean based on the established empirical relationship of -
341 0.0607 mmol/mol per 1°C derived from >30 published Sr/Ca calibrations (Corrège,
342 2006). This slope is well within the range of our regressions based on a variety of SST
343 datasets (Tab. A2). We use a conservative estimate for the uncertainty around relative
344 SST changes based on the difference between lower (-0.04) and upper slope (-0.084)

Biogeosciences Discuss., doi:10.5194/bg-2016-69, 2016
Manuscript under review for journal Biogeosciences
Published: 3 March 2016

345 estimates from these regression equations, thus ± 0.02 mmol per 1°C or ±0.33°C
346 (following Gagan et al., 2012; Tab. A2).

347 We validated the coral derived annual mean SST reconstruction against local Air
348 Temperature (AT), ERSSTv3b, ERSST4, HadISST, HadSST3 HadMAT1 and
349 HadNMAT2 for the period 1951 to 2006 (Figure 5; Figs. A4 to A6; See Supplementary
350 Tables 1-24 for mean annual correlations). The composite coral SST record clearly
351 follows instrumental SST in the grid box surrounding Rodrigues Island while the best fit
352 is obtained with local Rodrigues AT. Discrepancies with gridded SST products are
353 observed between 1951 and 1955. However, AT agrees with coral composite SST in that
354 period, yet not with core Cabri which tracks grid-SST between 1951 and 1955. However,
355 taking into account the uncertainty of ±0.33°C based on the regression error, coral
356 composite SST agrees with gridded SST within 1σ.

357 For the period 1951 to 2005, we used AT, ERSSTv3b, ERSST4, HadISST,
358 HadSST3, HadMAT1 and HadNMAT2 to validate trends in annual mean coral Sr/Ca-
359 SST anomalies (Fig. 5, 6). The long-term trends in Sr/Ca-derived SST anomalies for the
360 period 1951 to 2005 for Cabri and Totor converted to SST, using the published Sr/Ca-
361 SST relationship of -0.0607mmol/mol per 1°C, indicate a warming of 1.38±0.39°C and
362 cooling of -0.49±0.41°C, respectively. The composite Sr/Ca anomaly time series for 1951
363 to 2005 display a warming trend of 0.44±0.37°C. The uncertainty for the trend estimates
364 in coral Sr/Ca SST is calculated from the square root of the sum of squares of the
365 regression error and the error in the slope of the Sr/Ca-SST relationship. Instrumental
366 SST indicate a warming trend of 0.61±0.13°C for HadISST, 0.72±0.11°C for ERSST3b
367 (0.86±0.12°C for ERSST4) and 0.78±0.12°C for HadSST3. Air Temperature at

Biogeosciences Discuss., doi:10.5194/bg-2016-69, 2016
Manuscript under review for journal Biogeosciences
Published: 3 March 2016

368 Rodrigues weather station recorded a warming trend of 0.46±0.17°C. All trends are
369 significant at the 2% level with the exception of the negative trend in Sr/Ca SST
370 anomalies in the Totor core which is not significant.

371 For the pre-1945 period we used ERSSTv3b, HadSST1 and HadSST3 to validate
372 annual mean coral Sr/Ca-SST back to 1854 and 1870, respectively (Figure 6). We stress
373 that the number of SST observations in the ICOADS SST database is extremely sparse
374 for our region (Fig. A2). However, the composite coral SST record tracks SST variations
375 for most of the past 150 years (Figure 6). The composite coral SST time series,
376 essentially the time series of core Totor, displays higher SST anomalies compared to all
377 gridded SST reconstructions in the 1850's, between 1916-1921, 1936-1941 and 1948-
378 1951 and lower SST anomalies for brief periods between 1850 and 1890. In general, the
379 coral composite SST is a valid reconstruction for the region surrounding Rodrigues Island
380 with the possible exception of 1854-1860, 1916-1921, 1936-1941 and 1948-1951 (Figure
381 6).

382 Largest discrepancies between grid-SST (starting from year 1854) and coral SST
383 reconstructions are found for core Totor with warm anomalies in the periods 1854-1860,
384 1916-1921, 1936-1941 and 1948-1951 (Figure 6). Interestingly, the correlation between
385 Totor Sr/Ca-SST, which dominates the coral composite time series pre-1945, has
386 significant correlations with HadSST3 ($r=0.24$; $p=0.05$; $N=65$) and HadNMAT2 ($r=0.3$;
387 $p=0.014$; $N=64$) observational time series only. The cool bias in coral derived SST
388 between 1882 and 1887 (slab 7) is most probably related to diagenetic alterations, but
389 none of the anomalously warm periods can be explained by diagenesis (see next section).
390 We assessed the orientation of corallites to the coral slab surface to test for sampling

Biogeosciences Discuss., doi:10.5194/bg-2016-69, 2016
Manuscript under review for journal Biogeosciences
Published: 3 March 2016

artifacts that might have altered our Sr/Ca data which we summarized in Tables 2 and 3, illustrate in Figure 7 and discuss in section 6.1. Most anomalous warm periods show sub-optimal orientation of sampling path with corallites at an angle to the slab surface (see 6.1).

5.4 Diagenetic tests for alterations of Sr/Ca profiles

Representative samples for diagenetic screening with XRD, SEM and light microscopy were identified on the coral slabs using the X-radiographs. Additionally, intervals with presumably anomalous proxy values (warm or cold anomalies) were analyzed with the same methods. Ten thin-sections, six SEM samples, ten powder-XRD and thirteen spot-2D-XRD samples were analyzed from coral core Totor (Fig. 8). For coral core Capri, seven thin-sections, one powder-XRD and six 2D-XRD samples were analyzed. Neither powder nor spot-XRD analysis detected any calcite. Thin-section analysis indicates a growth break within slab 12 that is also apparent in the radiograph (Fig. 8; Fig. A7). Close to this break the coral is strongly affected by bioerosion and encrustation by red algae (Fig. 8ef). However, the sampling transect for geochemical analysis excluded this area and is therefore not affected by diagenesis (Fig. 8f). Combined SEM, EDS and XRD analysis shows low amounts of patchy distributed isopachous (~2µm) fibrous aragonite cement in slabs Totor 6 (1916-1921), 7 (1882-1887) and 11 (~ 1809).

Aragonite cement should lead to higher Sr/Ca values and lower reconstructed temperatures (Hendy et al., 2007). An interesting outcome is that the observed diagenesis is not able to explain the Sr/Ca ratios except for the slab Totor 7. Here the observed

Biogeosciences Discuss., doi:10.5194/bg-2016-69, 2016
Manuscript under review for journal Biogeosciences
Published: 3 March 2016

414 aragonite cement fits to relatively high Sr/Ca values resulting in a cold anomaly. No
415 anomalously high Sr/Ca ratios are associated with the patchy aragonite cements in slabs 6
416 and 11. Instead slabs 6 and 11 are characterized by low Sr/Ca ratios resulting in relatively
417 warm reconstructed temperatures. All other samples from the slabs Totor 3, 4, 8, 9 and 10
418 are devoid of diagenetic alteration. In summary, an influence of diagenesis on the proxy
419 record and resulting SST reconstructions can only be assumed for sample Totor 7 (years
420 1882-1887). Core Cabri showed only localized (single month) positive Sr/Ca anomalies
421 (cool SST bias). Thin-section and XRD analysis did not indicate any diagenetic
422 alteration, but the coral locally contained aragonitic sediment partially filling pore spaces
423 (Tab. 3). This aragonitic sediment potentially could have caused the isolated Sr/Ca peaks.
424 These individual data points were omitted from further analysis.
425
426 **5.5 Large scale teleconnections on interannual time scales**
427 For the period of most reliable data coverage between 1951 and 2006, the
428 detrended coral composite and Cabri Sr/Ca-SST records shows positive correlations for
429 austral summer and annual means with Indian Ocean wide SST and a positive correlation
430 with the central and eastern Pacific SST typical for the spatial ENSO and PDO pattern
431 (Figure 9; Supplementary Tables 24-25). We used HadISST (1870 and 2006) and
432 HadMAT1 to evaluate the long-tern spatial correlation pattern (Figs. A3 to A5). A similar
433 pattern emerged as for the period 1951 to 2006, yet of weaker magnitude across the
434 Pacific and confined to the southwestern Indian Ocean. We broke down the correlations
435 into 30 year segments starting in 1870 to test if the correlation changes throughout the
436 past 136 years. The ENSO/PDO pattern for austral summer is strong in the periods 1870-

Biogeosciences Discuss., doi:10.5194/bg-2016-69, 2016
Manuscript under review for journal Biogeosciences
Published: 3 March 2016

1900, 1961-1990 and 1971-2006 (Fig. A3). Between 1900 and 1930 the correlation is not significant. The large-scale teleconnections with SST are stronger for the Cabri Sr/Ca-SST time series after 1945 (Figs. A4, A5), while core Totor has weaker and statistically non-significant correlations in that period. This indicates that the Cabri time series is more reliable for the recent 60 years for monthly averages and annual means and shows the strongest correlations across the Indo-Pacific (Fig. 9; Figs. A4, A5; Supplementary Tables 25, 26).

For detrended mean annual time scales (July-June) and austral summer (JFM) the Cabri SST record shows a positive correlation with southern Indian Ocean SST along a southeast to northwest band stretching along the trade wind belt (Figure 9d-f; Fig. A4). The correlation with the southern Indian Ocean trade wind belt remains stable over different record length and is most pronounced post 1971. We also find positive correlations with the Bay of Bengal and the Maritime Continent throughout the past 60 years. We find positive correlations with the eastern Pacific SST and negative correlations with the northern Pacific along 40°N and stretching between 160°E and 150°W. The SST pattern mimics part of the typical spatial ENSO and PDO pattern across the Indo-Pacific (Mantua et al., 1997; McPhaden et al., 2006).

6 Discussion

6.1 Diagenesis, orientation of corallites and potential biases in Sr/Ca derived SST

Diagenesis could be excluded as a major cause of discrepancies between coral SST and grid-SST. For core Totor, only for the period between 1882 and 1887 we have to assume that diagenesis caused a cool bias on our coral SST reconstruction (Figure 8).

Biogeosciences Discuss., doi:10.5194/bg-2016-69, 2016
Manuscript under review for journal Biogeosciences
Published: 3 March 2016

460 Core Cabri showed only localized positive Sr/Ca anomalies (cool SST bias) most
461 probably caused by aragonitic sediment trapped within growth framework pores. These
462 samples have been removed before interpolation. Having excluded diagenesis for most of
463 the record, we assessed sampling biases due to changes in the orientation of growth axes
464 and positioning of corallites to the slab surface. De Long et al. (2012) showed clear
465 evidence for warm or cool biases in coral Sr/Ca-SST reconstructions caused by
466 suboptimal orientation of corallites in corals from New Caledonia. We have adopted a
467 similar approach to test for sampling biases in our two cores (Table 2 & 3). We found
468 that core Totor contained areas where a sampling bias could explain anomalous Sr/Ca-
469 derived SST. The warm anomaly between 1916 and 1921 with its peak values in 1919
470 stands out as the largest single anomaly in the record. However, diagenesis cannot
471 explain the warm anomalies. The growth rates and Sr/Ca seasonality for all years
472 between 1916 and 1921 are not anomalous and close to the average seasonality from *in*
473 *situ* SST data. The orientation of the corallites is mostly optimal (parallel to slab surface)
474 to the surface. However, for the years 1916 to 1921 we recognized an interval with
475 bundles of oblong corallites where our sampling transects switched from optimal to
476 suboptimal growth orientation. De Long et al. (2012) showed that warm biases were often
477 caused by corallites orientated at an angle or oblong to the slab surface and where growth
478 orientation had changed. These suboptimal intervals have seasonal cycles with more
479 summer Sr/Ca values than winter values causing an apparent warm bias. The latter could
480 not be identified for core Totor 1918-1919 values. Nevertheless, the extreme warm
481 anomaly between 1916 to 1921 is most likely related to the change in growth direction
482 associated with an unidentified vital effect. Interestingly, despite the potential influence

Biogeosciences Discuss., doi:10.5194/bg-2016-69, 2016
Manuscript under review for journal Biogeosciences
Published: 3 March 2016

of vital effects on the trend, the seasonality in this core section was well preserved. This implies that seasonality can be captured robustly while absolute values and trends are potentially biased by vital effects. This adds confidence for the study of seasonality from fossil corals where vital effects are harder to distinguish from true variability due to the lack of SST data for verification.

The warm anomalies in the periods 1854-1860, 1936-1941 and 1948-1951 in core Totor are all associated with an orientation of corallites at an angle to the slab surface. Yet, the interval 1936 to 1941 shows a high growth rate and normal seasonality in Sr/Ca for all years and no extreme over-representation of summer versus winter samples. The intervals 1948 to 1951 and 1854 to 1860 both showed reduced growth and seasonality which might have caused apparent warmer winter Sr/Ca values. We also detected areas with warm anomalies for years that predate instrumental data coverage (Tab. 2). The 1820's and 1830's likely have a warm bias due to corallites at an angle, disorganized fans and reduced growth rate with more summer values (Tab. 2). Between 1798 and 1816, the orientation is optimal and no bias can be inferred. The years pre-1798 have to be considered with caution since the bottom of the core Totor did show disorganized fans at places and/or suboptimal orientations pointing to likely warm biases (indicated in Figure 6).

Between 1984 and 2005 (core tops), Sr/Ca trends in cores Totor and Cabri deviate with Totor showing a cooling trend while Cabri shows a strong warming trend (Fig. 7). Our analysis of growth orientation revealed that the corallites in core Totor form parallel, elongated rods of septa for the entire period 1984 to 2005 (Fig. 7) while Cabri does show an optimal orientation of corallites for the core top between 1984 and 2006 (Fig. 7), with

Biogeosciences Discuss., doi:10.5194/bg-2016-69, 2016
Manuscript under review for journal Biogeosciences
Published: 3 March 2016

506 the exception of sub-optimal corallites in the period 2000 to 2006. The peculiar structure
507 of the corallites in Totor, at a first glance, would suggest optimal vertical growth of the
508 corallites with the polyps clearly visible from the apex of the core slab. However, this
509 structure is clearly associated with high Sr/Ca ratios and articifially cold SST anomalies.
510 A similar structure of the corallites was found in *Porites lutea* from St. Marie Island off
511 East Madagascar (core STM4 in Grove et al. 2013). Grove et al. (2013) ascribed the
512 Sr/Ca trend difference between cores STM2 and STM4 to changes in coral growth and
513 calcification, yet their results were not conclusive. Re-examination of core STM4
514 revealed that it also forms the parallel-elongated rods of septa in the core top, which was
515 biased towards high Sr/Ca ratios and therefore cold SST anomalies. STM4 also showed
516 low densities in this core top section that agrees with low density in Totor. Inspection of
517 various core sections in Totor and other coral cores revealed that similar elongated rods
518 of septa (not sampled down core) are formed between neighboring growth fans of septa.
519 We suggest that these parallel septa grow very fast in summer and winter, therefore show
520 no clear density contrast with overall low skeletal density. The Sr/Ca seasonality is also
521 strongly enhanced and samples contain a higher number of winter samples that record
522 high Sr/Ca ratios in Totor. Interestingly, the summer Sr/Ca values between cores Totor
523 and Cabri agree rather well between 1984 and 2005 while the winter values in Totor are
524 strongly biased to extreme cold anomalies. We suggest that core tops from *Porites* sp.
525 with similar parallel septa should be avoided for sampling since it can cause a cold bias in
526 Sr/Ca-based SST reconstructions.

527 Overall, our test for sampling biases to a large extend confirms the findings of De
528 Long et al. (2012) and indicates that such analysis should accompany climate

Biogeosciences Discuss., doi:10.5194/bg-2016-69, 2016
Manuscript under review for journal Biogeosciences
Published: 3 March 2016

529 reconstructions from coral cores. Our results suggest that a new core needs to be obtained
530 from the Totor colony or other large *Porites* sp. in order to overcome the SST biases
531 identified in the current record. The Cabri coral (>3.5m in height) would be an ideal site
532 since for the period 1945 to 2006 it provided an excellent and largely un-biased record of
533 SST. Yet, the 1907 dead surface was present in three long cores drilled from the Cabri
534 coral at different angles, which could undermine the SST reconstruction for a few
535 decades below the mortality event. The reason for the mortality event could not be
536 determined.
537
538 **6.2 SST trends and large-scale climate teleconnections since 1945**
539 Based on our analysis of corallite orientations, we conclude that core Cabri is
540 most likely the best representation to assess SST trends and interannual variability since
541 1945. Nevertheless, trend estimates in both individual cores and for the composite record
542 need to be interpreted with caution (as indicated in Figure 6).
543 Both, the Cabri and coral composite time series show an increase in SST over the
544 past 60 years (since 1945; Figs. 5 and 6). The Cabri time series recorded a higher SST
545 rise (1.38±0.41°C) than instrumental data, which ranged between 0.61 to 0.86±0.15°C,
546 and the composite coral record (0.44±0.37). The trend in Cabri agrees with all SST
547 datasets within 2σ, whereby the lower range of uncertainty for the Cabri trend estimates
548 (~1°C) and the upper range for the coral composite (~0.8°C) is in closes agreements to
549 trends from gridded SST datasets. Most of the accelerated warming trend in Cabri
550 resulted from the recent 6 years where the orientation of the corallites was sub-optimal.
551 The composite record agrees with the trend in AT at Rodrigues and marine AT

Biogeosciences Discuss., doi:10.5194/bg-2016-69, 2016
Manuscript under review for journal Biogeosciences
Published: 3 March 2016

552 (HadMAT1, HadNMAT2) within 1σ, yet likely underestimates the trend in grid-SST
553 (Fig. 5; Figs. A5, A6). The AT record shows very warm anomalies for the years 1951 to
554 1955 which resulted in a lower long-term trend. The composite record also showed warm
555 years between 1951 and 1955 due to core Totor that indicated warm SST while Cabri
556 followed grid SST with colder temperatures (Fig. 5). The Totor site is a sheltered location
557 with light winds and restricted water movement, with all three having contributed to
558 severe bleaching in 2002 at this site (Hardman et al., 2004, 2008). It could well be that
559 core Totor has at times recorded local SST variations that do not reflect open ocean
560 conditions or those at the more exposed site Cabri. This site-specific, local SST
561 variability might partly explain the high SST anomalies in Totor between 1936 and 1941
562 where the orientation of the corallites did not conclusively accounted for Sr/Ca-SST
563 anomalies. We conclude that the SST trend in Cabri and the coral composite closely
564 follows open ocean grid-SST which both indicate strong warming (~0.68-1°C) of the
565 south-central Indian Ocean over the past 60 years. Roxy et al. (2014) reported that during
566 1901–2012, the Indian Ocean warm pool warmed by 0.78°C while the western Indian
567 Ocean (5°S–10°N, 50°–65°E) experienced anomalous warming of 1.28°C in summer
568 SSTs. Our results for Cabri are therefore not unusual and within the range of observed
569 Indian Ocean SST trends (Annamalei et al., 2005; Alory et al., 2007; Koll Roxy et al.,
570 2014). The strong warming in the southern Indian Ocean trade wind belt could potentially
571 alter the monsoon circulation, especially during the monsoon onset phase in austral
572 autumn (March to May; Annamalei et al., 2005). Both, our coral SST time series and SST
573 products indicate the strongest warming for the March to May season (not shown).
574 Rodrigues station precipitation is strongly positively correlated with SST between March

Biogeosciences Discuss., doi:10.5194/bg-2016-69, 2016
Manuscript under review for journal Biogeosciences
Published: 3 March 2016

575 and May. When precipitation is anchored over a warmer SWIO between March and May
576 it can prevent the movements of the ITCZ towards the North and potentially disrupt the
577 Asian monsoon onset (Annamalei et al., 2005).

578 Both the Cabri and coral composite SST reconstructions revealed a clear
579 ENSO/PDO teleconnection pattern for mean annual and austral summer averages with
580 positive correlations across the Indian Ocean resembling the Indian Ocean basin mode
581 pattern (Xie et al., 2016) in response to ENSO and PDO (Fig. 9). Cabri shows the
582 strongest teleconnection pattern, which suggests that this time series is the most reliable
583 between 1945 and 2006 to assess ENSO/PDO impacts on Rodrigues (Figs. A3 to A5).
584 The ENSO/PDO teleconnection was stable for the recent 60 years, yet was strongest
585 between 1971 and 2006 (Fig. 9c,f). The latter period is known for increased occurrence of
586 El Niño events and a switch to a positive PDO phase up to 1999 (McPhaden et al., 2006).
587 These results are in agreement with ENSO/PDO pattern correlations observed in other
588 coral records from the southwestern Indian Ocean (Pfeiffer et al., 2004; Crueger et al.,
589 2009). However, this is the first Indian Ocean coral SST reconstruction that shows a clear
590 relationship with the PDO, while other coral records reflected PDO relationships with
591 rainfall/river runoff (Grove et al., 2013) and salinity/sea level pressure (Crueger et al.,
592 2009; Pfeiffer et al., 204).

593 Coral reefs of Rodrigues escaped the mass coral bleaching event of the 1997–
594 1998 El Niño, yet experienced bleaching in February 2002, March-April 2005 and April-
595 May 2006 (Hardman et al., 2004, 2008). The most severely affected sites with highest
596 coral mortality were located in the north and west of the island with our site Totor located
597 within the zone of most severely affected reefs in 2002, 2005 and 2006 (Hardman et al.,

Biogeosciences Discuss., doi:10.5194/bg-2016-69, 2016
Manuscript under review for journal Biogeosciences
Published: 3 March 2016

598 2004, 2008). Our site Cabri showed only 11-30% bleached corals in 2005, yet less severe
599 impacts in 2006 and 2007 and appears less frequently impacted by anomalously high SST
600 during recent El Niño events. Hardman et al. (2008) concluded that coral bleaching at
601 Rodrigues is very patchy and to date most sites appear to be resilient to current El Niño
602 thermal stress events. The relatively large seasonal SST amplitude (6.22°C) and high
603 standard deviation (2.14°C) might serve as buffer to prevent extended periods of thermal
604 stress events during El Niño events. Degree heating weeks for Rodrigues post 1998 rarely
605 exceeded 4 weeks and only in 2002 and 2005 reached 8 weeks at the northern and north-
606 western coral reef sites which have experienced severe thermal stress and are in decline
607 (Hardman et al., 2008). Despite the strong warming trend and El Niño related thermal
608 stress observed in our study, the corals of Rodrigues appear to be a safe haven for coral
609 survival. However, expected levels of future warming in the coming decades will
610 increase thermal stress levels and probably increase coral bleaching and mortality.
611 Rodrigues receives a very limited larval supply suggesting that the reefs rely on larval
612 retention and self-seeding for population recovery. Gilmour et al. (2013) and Graham et
613 al. (2015) showed that isolated reefs with limited larval supply might be the more
614 susceptible to climate change-driven reef degradation, despite escaping many of the
615 stressors impacting continental reef systems. It is therefore most important to reduce local
616 stressors at Rodrigues to provide the corals enough time to bounce back after thermal
617 stress disturbance.
618
619 **7 Conclusions**

Biogeosciences Discuss., doi:10.5194/bg-2016-69, 2016
Manuscript under review for journal Biogeosciences
Published: 3 March 2016

620 We reconstruct SST for Rodrigues Island located in the south-central Indian Ocean trade
621 wind belt. Our reconstruction is based on two monthly-resolved coral Sr/Ca records
622 (Totor, Cabri) from Rodrigues Island (63°E, 19°S) that extend to 1781 and 1945,
623 respectively. We identify potential biases in our SST reconstructions associated with the
624 orientation of the corallites and conclude that careful screening for diagenesis and
625 orientation of corallites is of paramount importance to ensure high quality of Sr/Ca-based
626 SST reconstructions. However, our proxy records provide the most reliable SST
627 reconstruction between 1945 and 2006 and for several multi-decadal periods over the past
628 224 years. Reconstructed long-term SST trends are within the range of trends reported
629 from observational SST data for the western Indian Ocean. Furthermore, we identify
630 teleconnections with the ENSO/PDO over the past 60 years, eg. warming of SST during
631 El Niño or positive PDO. Our reconstruction is the first coral proxy record for SST that
632 shows a relationship with the PDO spatial correlation pattern in SST. We suggest that
633 Rodrigues Island is an ideal site to assess SST variations in the southern Indian Ocean
634 trade wind belt and their climatic teleconnection with the ENSO/PDO on longer time
635 scales.
636

637 **8 Acknowledgements**

638 The coral paleoclimate work was supported as part of the SINDOCOM grant
639 under the Dutch NWO program 'Climate Variability', grant 854.00034/035. Additional
640 support comes from the NWO ALW project CLIMATCH, grant 820.01.009, and the
641 Western Indian Ocean Marine Science Association through the Marine Science for
642 Management program under grant MASMA/CC/2010/02. We thank the team of

643 SHOALS Rodrigues for their excellent support in fieldwork logistics and in the
644 organization of the research and CITES permits. We would also like to thank the
645 Rodrigues Assembly and the Ministry for Fisheries for granting the research and CITES
646 permits. A Senior Curtin Fellowship in Western Australia, and an Honorary Fellowship
647 with the University of the Witwatersrand, South Africa, supported JZ. Bouke Lacet and
648 Wynanda Koot (VUA) helped cut the core slabs and prepared the thin sections. Janice
649 Lough and Eric Matson (AIMS) provided skilled technical support for coral core
650 densitometry measurements and data processing. We thank Dieter Garbe-Schoenberg for
651 assistance with the ICP-OES measurements.

652

653 **References**

654 Alibert, C. and McCulloch M. T.: Strontium/calcium ratios in modern Porites corals from the
655 Great Barrier Reef as a proxy for sea surface temperature: calibration of the thermometer and
656 monitoring of ENSO, Paleoceanography, 12(3), 345-363, 1997.
657
658
659 Alory, G. and Meyers, G.: Warming of the Upper Equatorial Indian Ocean and Changes in the
660 Heat Budget (1960–99), J. Climate, 22, 93–113, 2009.
661
662 Annamalai, H., Liu, P. and Xie, S.-P.: Southwest Indian Ocean SST Variability: Its Local
663 Effect and Remote Influence on Asian Monsoons, Journal of Climate, 18, 4150-4167, 2005.
664
665 Carricart-Ganivet, J. P. and Barnes D. J.: Densitometry from digitized images of X-
666 radiographs: methodology for measurement of coral skeletal density, Journal of Experimental
667 Marine Biology and Ecology, 344, 67-72, 2007.
668
669 Charles, C. D., Hunter, D. E. and Fairbanks R. G.: Interaction between the ENSO and the Asian

Monsoon in a coral record of tropical climate, Science, 277, 925-928, 1997.

Cobb, K. M., Charles, C. D. and Hunter D. E.: A central tropical pacific coral demonstrates pacific, Indian, and Atlantic decadal climate connections, Geophysical Research Letters 28(11), 2209-2212, 2001.

Cole, J. E., Dunbar, R. B., McClanahan, T. R. and Muthiga N. A.: Tropical Pacific forcing of decadal SST variability in the Western Indian Ocean over the past two centuries. Science 287, 617-619, 2000.

Corrège, T.,: Sea surface temperature and salinity reconstruction from coral geochemical tracers. Palaeogeo. Palaeoclim. Palaeoeco., 232, 408-428, 2006.

Crueger, T., Zinke, J. and Pfeiffer M.: Patterns of Pacific decadal variability recorded by Indian Ocean corals. International Journal of Earth Sciences 98, doi:10.007/s00531-00008-00324-00531, 2009.

DeLong, K. L., Quinn, T. M., Taylor, F. W., Shen, C.-C. and Lin, K.: Improving coral-base paleoclimate reconstructions by replicating 350 years of coral Sr/Ca variations, Palaeogeography, Palaeoclimatology, Palaeoecology, 373, 6-24, 2013.

DeVilliers, S., Sheng, G.T., Nelson, B.K.: The Sr /Ca-temperature relationship in coralline aragonite: Influence of variability in (Sr/Ca)seawater and skeletal growth parameters, Geochimica et Cosmochimica Acta, 58, 197-208, 1994.

Felis, T. and Paetzold, J.: Climate records from corals, In: Marine Science Frontiers for Europe. Eds.: G. Wefer, F. Lamy and F. Mantoura. Berlin, Heidelberg, New York, Tokyo, Spinger, p. 11-27, 2003.

Funk, C., Dettinger, M. D., Michaelsen, J. C., Verdin, J. P., Brown, M. E., Barlow, M. and Hoell, A.: Warming of the Indian Ocean threatens eastern and southern African food security

701 but could be mitigated by agricultural development, Proceedings Nat. Acad. Sci., 105(32),
702 11081-11086, 2008.
703
704 Gagan, M. K., Dunbar, G. B. and Suzuki, A.: The effect of skeletal mass accumulation in
705 Porites on coral Sr/Ca and d18O paleothermometry, Paleoceanography 27, PA1203,
706 doi:10.1029/2011PA002215, 2012.
707
708 Gilmour, J.P., Smith, L.D., Heyward, A.J., Baird, A.H., Pratchett, M.S.: Recovery of an
709 isolated coral reef system following severe disturbance, Science, 340, 69–71, 2013.
710
711 Graham, N.A.J., Jennings, S.M., MacNeil, M.A., Mouillot, D., Wilson, S.K.: Predicting
712 climate-driven regime shifts versus rebound potential in coral reefs, Nature, 518, 94-97, 2015.
713
714 Grove, C. A., Kasper, S., Zinke, J., Pfeiffer, M., Garbe-Schönberg, D. and Brummer, G.-J. A.:
715 Confounding effects of coral growth and high SST variability on skeletal Sr/Ca: Implications
716 for coral paleothermometry, Geochem., Geophys. Geosyst., 14, doi:10.1002/ggge.20095, 2013.
717
718 Grove, C. A., Zinke, J., Peeters, F., Park, W., Scheufen, T., Kasper, S.,
719 Randriamanantsoa, B., McCulloch, M. T. and Brummer, GJA (2013). Madagascar corals
720 reveal multidecadal modulation of rainfall since 1708. Climate of the Past 9, 641-656.
721
722 Hardman, E. R., Meunier, M. S., Turner, J. R., Lynch, T. L., Taylor, M. and Klaus R.: The
723 extent of coral bleaching in Rodrigues, Journal of Natural History, 38, 3077-3089, 2004.
724
725 Hardman, E. R., Stampfli, N. S., Hunt, L., Perrine, S., Perry, A. and Raffin, J. S.: The Impacts
726 of coral bleaching in Rodrigues, Western Indian Ocean, Atoll Research Bulletin, 555, DOI:
727 10.5479/si.00775630.555.1, 2008.
728
729 Helmle, K. P., Dodge, R.E., Swart, P.K., Gledhill, D.K. and Eakin, C.M.: Growth rates of
730 Florida corals from 1937 to 1996 and their response to climate change, Nat. Commun, 2, 215
731 doi: 10.1038/ncomms1222, 2011.

Hendy, E. J., Gagan, M. K., Lough, J. M., McCulloch, M., and deMenocal P. B.: Impact of skeletal dissolution and secondary aragonite on trace element and isotopic climate proxies in Porites corals, Paleoceanography, 22, PA4101, doi:10.1029/2007PA001462, 2007.

Kaplan, A. *et al.* Analyses of global sea surface temperature 1856-1991, J. Geophys. Res., 103, 18567-18589, 1998.

Kennedy J.J., Rayner, N.A., Smith, R.O., Saunby, M. and Parker, D.E.: Reassessing biases and other uncertainties in sea-surface temperature observations since 1850 part 1: measurement and sampling errors, J. Geophys. Res., 116, D14103, doi:10.1029/2010JD015218, 2011.

Kent, E.C., Rayner N.A., Berry D.I., Saunby M., Moat B.I., Kennedy J.J., Parker D.E.: Global analysis of night marine air temperature and its uncertainty since 1880: the HadNMAT2 Dataset, Journal of Geophys. Res., doi: 10.1002/jgrd.50152, 2013.

Koll Roxy, M., Ritika, K., Terray, P., Masson, S.: The curious case of Indian Ocean warming, Journal of Climate 27, 8501-8509, 2014.

Lee, S.-K., Park, W., Baringer, M. O., Gordon, A. L., Huber, B. and Liu ,Y.: Pacific origin of the abrupt increase in Indian Ocean heat content during the warming hiatus, Nature Geoscience, 8, 445-449, 2015.

Lynch T.L., Meunier, M.S., Hooper, T.E.J., Blais, F.E.I., Raffin, J.S.J, Perrine, S., Félicité, N., Lisette, J., Grandcourt, J.W.: Annual report of benthos, reef fish and invertebrate surveys for Rodrigues 2002, Shoals Rodrigues report, 30pp, 2002.

Mantua, N. J., Hare, S. R., Zhang, Y., Wallace, J. M., and Francis, R. C.: A Pacific decadal climate oscillation with impacts on salmon, Bull. Amer. Meteor. Soc., 78, 1069–1079, 1997.

762 Mart, Y.: The tectonic setting of the Seychelles, Mascarene and Amirante plateaus in the
763 Western Equatorial Indian ocean, Marine Geology, 79, 261-274, 1988.
764
765 McGregor H. V. and Gagan M. K.: Diagenesis and geochemistry of Porites corals from Papua
766 New Guinea: implications for paleoclimate reconstruction, Geochim. Cosmochim. Acta, 67,
767 2147–2156, 2003.
768
769 McGregor, H. V. and Abram, N. J.: Images of diagenetic textures in Porites corals from Papua
770 New Guinea and Indonesia, Geochemistry, Geophysics, Geosystems 9(10),
771 doi:10.1029/2008GC002093, 2008.
772
773 McPhaden, M. J., Stephen E. Zebiak, S. E., Glantz, M. H.: ENSO as an Integrating Concept in
774 Earth Science, Science, 314, 1740-1745, 2006.
775
776 Nakamura, N., Kayanne, H., Iijima, H., McClanahan, T. R., Behera, S. K. and Yamagata, T.:
777 Mode shift in the Indian Ocean climate under global warming stress, Geophysical Research
778 Letters, 36, L23708, doi:10.1029/2009GL040590, 2009.
779
780 New A. L., Alderson S. G., Smeed D.A., Stansfield K.L.: On the circulation of water masses
781 across the Mascarene Plateau in the South Indian Ocean, *Deep-Sea Research I* 54, 42–74, 2007.
782
783 New A. L., Stansfield, K., Smythe-Wright, D., Smeed D. A., Evans, A. J. and Alderson, S. G.:
784 Physical and biochemical aspects of the flow across the, Mascarene Plateau in the Indian
785 Ocean, *Philosophical Transactions of the Royal Academic Society* 363, 151–168, 2005.
786
787 Paillard, D., Labeyrie, L., Yiou, P.: Macintosh program performs time series analysis. Eos
788 Trans AGU 77, 379, 1996.
789
790 Pfeiffer, M., Timm, O. and Dullo, W.-C.: Oceanic forcing of interannual and multidecadal
791 climate variability in the southwestern Indian Ocean: Evidence from a 160 year coral isotopic

792 record (La Reunion, 50E, 21S). Paleoceanography, 19, PA4006, doi:10.1029/2003PA000964,
793 2004.
794
795 Pfeiffer, M., Timm, O., Dullo, W.-C. and Garbe-Schoenberg, D.: Paired coral Sr/Ca and d18O
796 records from the Chagos Archipelago: Late twentieth century warming affects rainfall
797 variability in the tropical Indian Ocean, Geology, 34(12), 1069-1072, 2006.
798
799 Pfeiffer, M., Dullo, W.-C., Zinke, J. and Garbe-Schoenberg, D.: Three monthly coral Sr/Ca
800 records from the Chagos Archipelago covering the period of 1950-1995 A.D.: reproducibility
801 and implications for quantitative reconstructions of sea surface temperature variations,
802 International Journal of Earth Sciences, 98, doi:10.007/s00531-00008-00326-z, 2009.
803
804 Rayner, N. A., Parker, D. E., Horton, E. B., Folland, C. K., Alexander, L. V., Rowell, D. P.,
805 Kent, E. C. and Kaplan A.: Global analyses of sea surface temperature, sea ice, and night
806 marine air temperature since the late nineteenth century. Journal of Geophysical Research
807 **108**(D14), doi:10.1029/2002JD002670, 2003.
808
809 Reynolds, R.W., Rayner, N.A., Smith, T.M., Stokes, D.C., Wang W.: An improved in situ and
810 satellite SST analysis for climate, Journal of Climate, 15, 1609–1625, 2002.
811
812 Reynolds, R. W., Smith, T. M., Liu, C., Chelton, D. B., Casey, K. S. and Schlax, M. G.: Daily
813 high-resolution blended analyses for sea surface temperature, J. of Climate, 20, 5473-5496,
814 2007.
815
816 Sayani, H. R., Cobb, K. M., Cohen, A. L., Crawford Elliott, W., Nurhati, I. S., Dunbar, R. B.,
817 Rose, K. A., Zaunbrecher, L. K.: Effects of diagenesis on paleoclimate reconstructions from
818 modern and young fossil corals, Geochimica et Cosmochimica Acta, 75, 6361–6373, 2011.
819
820 Schott, F.A., McCreary, J.P.: The monsoon circulation of the Indian Ocean, Progress in
821 Oceanography, 51, 1–123, 2001.
822

Biogeosciences Discuss., doi:10.5194/bg-2016-69, 2016
Manuscript under review for journal Biogeosciences
Published: 3 March 2016

823 Schrag, D.P.: Rapid analyses of high-precision Sr/Ca ratios in corals and other marine
824 carbonates, Paleoceanography, 14, 2, 97-102, 1999.
825
826 Sepulcre, S., Durand, N., Bard, E.: Mineralogical determination of reef and periplatform
827 carbonates: calibration and implications for paleoceanography and radiochronology, Global
828 Planet Change, 66(1–2), 1–9, 2009.
829
830 Smith, T.M., Reynolds, R.W., Peterson, T.C., Lawrimore, J.: Improvements to NOAA's
831 historical merged land–ocean surface temperature analysis (1880–2006), J. of Climate, 21,
832 2283, 2008.
833
834 Smodej, J., Reuning, L., Wollenberg, U., Zinke, J., Pfeiffer, M. and Kukla, P. A.: Two-
835 dimensional X-ray diffraction as a tool for the rapid, nondestructive detection of low calcite
836 quantities in aragonitic corals, Geochemistry, Geophysics, Geosystems, 16,
837 10.1002/2015GC006009, 2015.
838
839 Tokinaga, H., Xie, S.P., Deser, C., Kosaka, Y., Okumura, Y. M.: Slowdown of the
840 Walker circulation driven by tropical Indo-Pacific warming. Nature, 491, 439-444, 2012.
841
842 Turner, J. and Klaus, R.: Coral reefs of the Mascarenes, Western Indian Ocean, Philosophical
843 transactions of the Royal Academic Society, 363, 229–250, 2005.
844
845 van Oldenborgh, G. J., Burgers, G.: Searching for decadal variations in ENSO
846 precipitation teleconnections, Geophys. Res. Lett., 32, L15701, 2005.
847
848 Woodruff, S.D. *et al.*: ICOADS Release 2.5: Extensions and enhancements to the surface
849 marine meteorological archive, Int. J. Climatol., 31, 951-967, 2011.
850
851 Xie, S.-P., Kosaka Y., Du Y., Hu K. M., Chowdary J. S., and Huang G.: Indo-western Pacific
852 ocean capacitor and coherent climate anomalies in post-ENSO summer: A review, Adv. Atmos.
853 Sci., 33(4), 411–432, 2016.

Biogeosciences Discuss., doi:10.5194/bg-2016-69, 2016
Manuscript under review for journal Biogeosciences
Published: 3 March 2016

Zinke, J., Pfeiffer, M., Park, W., Schneider, B., Reuning, L., Dullo, W.-Chr., Camoin, G. F., Mangini, A., Schroeder-Ritzrau, A., Garbe-Schönberg, D. and Davies, G. R.: Seychelles coral record of changes in sea surface temperature bimodality in the western Indian Ocean from the Mid-Holocene to the present, Climate Dynamics, 43 (3), 689-708, 2014.

Appendix A – Coral growth data and comparison to instrumental temperature records

Tables

Core name	GPS position	Species	Water depth (m)	Mean growth rate cm year^{-1}	Mean density g/cm^3	Mean Calcification rate g/cm^2 year^{-1}
Totor	S19º40.237; E63º25.754	*Porites sp.*	4.0	0.92 (±0.19)	1.128 (±0.11)	1.07 (±0.18)
Cabri	S19°40.030, E63°26.065	*Porites lobata*	3.0	1.18 (±0.25)	1.36 (±0.12)	1.60 (±0.16)

Table 1 - Coral cores with their GPS co-ordinates and depths at low tide, with mean rates of extension, densities and calcification over the complete length of the individual records.

Biogeosciences Discuss., doi:10.5194/bg-2016-69, 2016
Manuscript under review for journal Biogeosciences
Published: 3 March 2016

Section	Year	Orientation	Bias	Notes
1	2005-1987	Sub-optimal	cool	Corallites parallel to surface, yet straight angle; probably like a valley
2	1987-1982	Sub-optimal	cool	Corallites parallel to surface, yet straight angle; probably like a valley
2	1981-1977	Sub-optimal	warm	Corallites at an angle to the surface; oblong corallites
3	1978-1975	Sub-optimal	warm	Corallites at an angle to the surface
3	**1974-1958**	**Optimal**	**none**	**Corallites parallel to surface**
4A	1958-1952	Sub-optimal	warm	Corallites at an angle to the surface; scallop texture from angles of corallites
4A	1951-1945	Sub-optimal	warm	Corallites at an angle to the surface; 1947-1952 low growth rate; reduced seasonality
4B	**1947-1936**	**Optimal**	**none**	**Corallites parallel to surface, 1945-1947 better orientation than in slab 4A**
4B	**1938-1933**	**Sub-optimal**	**none**	**Corallites at an angle to the surface; 1936-1941 warm anomaly years show normal seasonality and high growth rate**
5	**1933-1922**	**Optimal**	**none**	**Corallites parallel to surface; 1922-1928 reduced seasonality**
6	1921-1915	Sub-optimal	warm	1915-21 warm spikes shows slightly oblong corallites, yet normal seasonality; switch from optimal to sub-optimal orientation
6	**1915-1896**	**Optimal to sub-optimal**	**none**	**Corallites mostly parallel to surface, small section with corallites at slight angle;;**
7	**1897-1890**	**Optimal**	**none**	**Corallites parallel to surface**
7	1887-1882	Optimal	cool	Diagenesis detected between years 1882-1887
7	**1881-1872**	**Sub-optimal**	**none**	**Corallites at an angle to the surface; 1872 close to bioerosion track; 1878-1880 low seasonality, yet no effect**
8	1872-1868	Sub-optimal	cool	Corallites at an angle to the surface; some corallites at almost 90° angle; 1868-1872 below bioerosion track; 1867-1871 low seasonality
9	1860-1854	Sub-optimal	warm	Corallites at an angle to the surface; 1854-1858 low seasonality, less winter samples
9	1856-1845	Sub-optimal	warm	Corallites parallel to surface; low seasonality with relatively warm winter samples
9	**1844-1831**	**Optimal**	**none**	**Corallites parallel to surface; only 1831-1832 corallites at an angle to surface**
10	1830-1827	Sub-optimal	warm	Corallites at an angle to the surface; oblong orientation
10	1826-1823	Disorganised	warm	Corallites rotating at 90° angle; low growth rate, seasonality reduced 1823-1825 with relatively warm winter samples
10	**1822-1815**	**Optimal**	**none**	**Corallites parallel to surface; low growth rate; reduced seasonality 1818-1822, yet no effect on SST anomalies**
11	**1816-1806**	**Sub-optimal**	**none**	**Corallites at an angle to the surface, yet no effect on SST anomalies**
11	**1807-1798**	**Sub-optimal**	**none**	**Corallites at an angle to the surface in sub-optimal parts; Corallites rotating at 90° angle near terminating fans (not sampled); 3 growth axes with terminating fans in between (not sampled); 1799-1807 regular seasonality**
11	1797-1792	Sub-optimal	warm	Corallites at an angle to the surface
12	1795-1792	Disorganised	warm	Corallites rotating at 90° angle; 1792-1791 long year, more summer samples
12	1791-1784	Sub-optimal	warm	Corallites parallel to surface; 1784-1787 Corallites at an angle to the surface; 1789-1794 seasonality distorted
12	1781-1783	Disorganised	warm	Corallites rotating at 90° angle; seasonality slightly distorted, apparently more summer samples

874 Table 2 – Summary of sampling issues detected in core Totor. Unbiased sampling tracks
875 indicated in bold.

Biogeosciences Discuss., doi:10.5194/bg-2016-69, 2016
Manuscript under review for journal Biogeosciences
Published: 3 March 2016

Section	Year	Orientation	Bias	Notes
1	2007-2000	Sub-Optimal	warm	Corallites parallel to surface; yet no clear growth fans
1	**1999-1992**	**Optimal**	**none**	**Corallites parallel to surface**
2	**1984-1992**	**Sub-optimal**	**none**	**Corallites at an angle to the surface; oblong corallites**
3	**1983-1968**	**Sub-Optimal**	**none**	**Corallites parallel to surface; yet no clear growth fan**
4	**1967-1964**	**Sub-optimal**	**none**	**Corallites at an angle to the surface**
5	**1963-1958**	**Optimal**	**none**	**Corallites parallel to surface**
5	**1957-1954**	**Sub-optimal**	**none**	**Corallites at an angle to the surface**
5	**1953-1945**	**Optimal**	**none**	**Corallites parallel to surface**

Table 3 – Summary of sampling issues detected in core Cabri. Unbiased sampling tracks indicated in bold.

Figure captions

Figure 1 – Map of Rodrigues island with the position of the two corals cores at Totor and Cabri indicated. The star shows the position of the CTD that collects SST and salinity data. Polygon indicates the location of the Meteorological Station which records air temperature, sunshine hours, wind speed and rainfall.

Figure 2 – Climatology at Rodrigues between 1997 to 2007. A) SST *in situ*, ERSSTv.3 (Smith et al., 2008) and AVHRR SST from NOAA Coral Reef Watch (Reynolds et al., 2007); b) air temperature and sunshine hours at Rodrigues Meteorological Station (MET); c) monthly averaged wind speed at MET.

Figure 3 – a) Time series of monthly (thin solid lines) Sr/Ca anomalies (right Y-axis) relative to the 1961 to 1990 climatological mean for coral cores Cabri (top), Totor (middle) and Coral composite (bottom) for the period 1781 to 2006.

Biogeosciences Discuss., doi:10.5194/bg-2016-69, 2016
Manuscript under review for journal Biogeosciences
Published: 3 March 2016

Figure 4 – Reconstructed absolute SST from coral Sr/Ca from cores Totor and Cabri for 2002 to 2006 based on calibration with in situ SST from Rodrigues. The uncertainty for single month absolute SST for individual cores Cabri and Totor is 1.23°C and 1.05°C (1σ), respectively. The coral data agree with *in situ* SST within the 1σ uncertainty.

Figure 5 – Time series of annual mean temperatures anomalies relative to the 1961-1990 mean for the coral composite SST, Rodrigues weather station Air temperature (AT), ERSSTv3b, ERSSTv4 , HadISST, HadSST3, HadMAT1 and HadNMAT2 for the period 1950 to 2006. The uncertainty of mean annual coral Sr/Ca-SST anomalies are indicated by the grey envelope.

Figure 6 – Annual mean time series of coral time series (red) for a) Cabri, b) Totor and c) the coral composite SST compared to SST reconstructions: ERSSTv3b, ERSSTv4, HadISST, HadSST3, HadMAT1 and HadNMAT2. See legend in a) for colours. For all time series we computed anomalies relative to 1961 to 1990. The uncertainty of mean annual coral Sr/Ca-SST anomalies are indicated by the grey envelope. Potential warm bias in coral SST is indicated by faint red shading, while cool bias by light blue shading. Yellow marks core intervals with diagenesis.

Figure 7 – a) Monthly interpolated Sr/Ca profiles for cores Cabri (red) and Totor (grey). B) Images of core Totor (coloured blue) with orientation of corallites indicated. Years for core sections indicated on coral slab and grey arrow points to major change in orientation of corallites in core top section of Totor around 1983/84.

Biogeosciences Discuss., doi:10.5194/bg-2016-69, 2016
Manuscript under review for journal Biogeosciences
Published: 3 March 2016

919

920 Fig. 8: Thin-section and scanning electron microscope (SEM) images. Thin section
921 photographs are shown in plane- (left) and cross-polarized light (middle). A and B:
922 Excellent preservation of coral skeleton without dissolution or cementation is typical for
923 the corals Totor and Cabri. Small patches of aragonite cements occur in parts of slab 6
924 (C), 7 (D) and 11 (E) of Totor. F (left): A prominent growth break visible in the
925 radiograph of slab 12 of Totor is characterized by abundant microborings and
926 encrustation by coralline red algae. F (middle): The section above the growth break is
927 well preserved. F (right): The coral core Cabri shows excellent preservation, only locally
928 containing aragonitic sediment partially filling pore spaces.
929

930 Figure 9 – Spatial correlation of Cabri Sr/Ca-SST anomalies (relative to 1961-1990) with
931 HadISST (Rayner et al., 2003). January to March austral summer in a) between 1945-
932 2006, b) 1961-1990 and c) 1971-2006. Annual mean correlations in d) between 1945-
933 2006, e) 1961-1990 and f) 1971-2006. Only correlation with $p<0.05$ are coloured.
934 Computed at knmi climate explorer (van Oldenborgh and Burgers, 2005).
935

936 Figure A1 – Relative changes in coral growth parameters (anomalies relative to 1961-
937 1990) of cores Totor (dark grey; since 1836) and Cabri (light grey; since 1907) versus
938 Rodrigues coral composite SST (black solid line) for period of best geochemical data
939 coverage.
940

941 Figure A2 –Number of SST observations in the grid box surrounding Rodrigues in the
942 ICOADS database. Note the extremely sparse observations even in recent years (van
943 Oldenborgh and Burgers, 2005).
944

Biogeosciences Discuss., doi:10.5194/bg-2016-69, 2016
Manuscript under review for journal Biogeosciences
Published: 3 March 2016

945 Figure A3 – Spatial correlations of global austral summer HadISST for 30-year periods
946 with a-f) austral summer coral composite summer SST (January to March) for different
947 30-year periods. Only correlations with p<0.05 coloured. Computed at knmi climate
948 explorer (van Oldenborgh and Burgers, 2005).
949
950 Figure A4 – Spatial correlations of Cabri coral SST with global austral summer HadISST
951 for a-c) 1950 to 1975 (February to May) negative PDO phase (Mantua et al., 1997) and c-
952 d) 1976 to 1999 (January to April) positive PDO phase. Only correlations with p<0.05
953 coloured. Computed at knmi climate explorer (van Oldenborgh and Burgers, 2005).
954 Figure A5 – Spatial correlations of mean annual HadMAT1 air temperature anomalies
955 between 1945 to 2001 relative to 1961-1990 with a) HadISST for Rodrigues, b) coral
956 composite SST and c) Cabri SST. Only correlations with p<0.05 coloured. Computed at
957 knmi climate explorer (van Oldenborgh and Burgers, 2005). Y-axis Latitude, X-axis
958 Longitude.
959
960 Figure A6 – Coral composite monthly SST anomalies relative to 1961-1990 (red)
961 compared to 5°x5° gridded HadNMAT2 night marine air temperature (blue; Kent et al.,
962 2013). The uncertainty of coral SST based on the regression slope error is indicated by
963 the grey envelope. Note the excellent agreement between the monthly anomalies.
964 Summer (Dec-April) and Winter (June-August) anomalies are correlated with r=0.5,
965 p<0.001 (N=56).
966

Biogeosciences Discuss., doi:10.5194/bg-2016-69, 2016
Manuscript under review for journal Biogeosciences
Published: 3 March 2016

967 Figure A7 – X-ray positive print for slabs of core Totor with sampling lines indicated.
968 Blue lines indicate high resolution sampling tracks. Yellow lines superimposed on blue
969 lines indicate sampling at annual resolution for other purposes. Start or end years for each
970 slab indicated.
971
972 Figure A8 - X-ray positive print for slabs of core Cabri with sampling lines (milling
973 holes) indicated. Start or end years for each slab indicated. Note the dead surface before
974 1907 that is most probably related to a past coral bleaching event.
975
976 Table A1 – Statistics of various sea surface temperature (SST) products and air
977 temperature for Rodrigues with 1σ standard deviations in brackets for the period 2002 to
978 2006 (period with *in situ* SST data). STDV = 1σ standard deviation over all years. All
979 units in °C.
980
981 Table A2 - Linear regression of coral Sr/Ca with a) *in situ* SST 2002-2005/6, b)
982 ERSSTv.3 (Smith et al., 2008) 1997-2005/6, c) AVHRR SST NOAA Coral Reef watch
983 data 2000-2005/6 and d) monthly Sr/Ca with AVHRR SST (Reynolds et al., 2007) for the
984 period 1982 to 2005.
985
986
987
988
989

Biogeosciences Discuss., doi:10.5194/bg-2016-69, 2016
Manuscript under review for journal Biogeosciences
Published: 3 March 2016

990 **Figures**

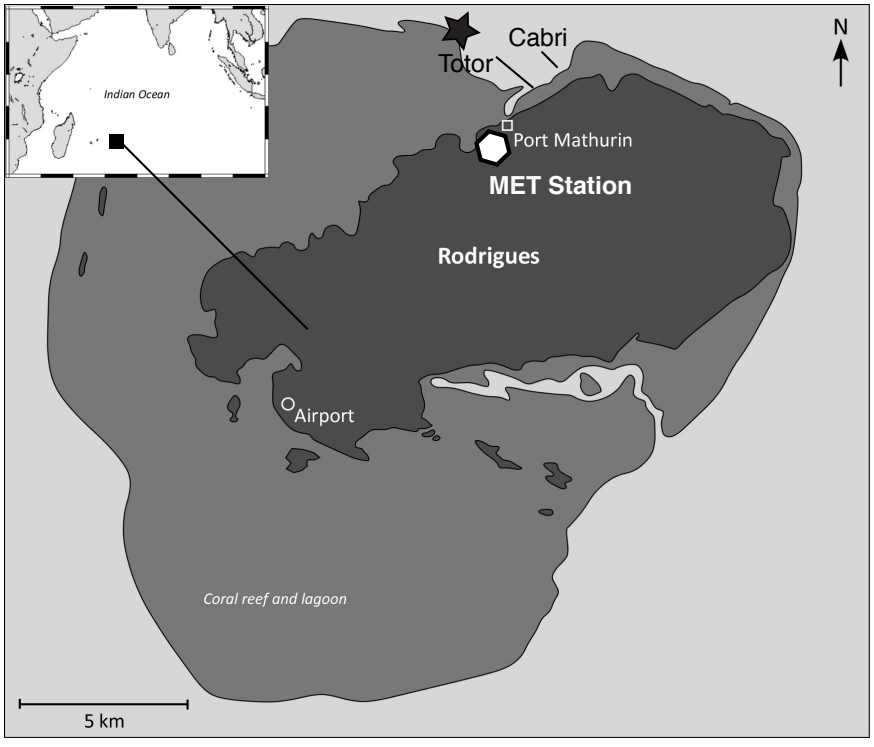

991

992 Figure 1

993

Biogeosciences Discuss., doi:10.5194/bg-2016-69, 2016
Manuscript under review for journal Biogeosciences
Published: 3 March 2016

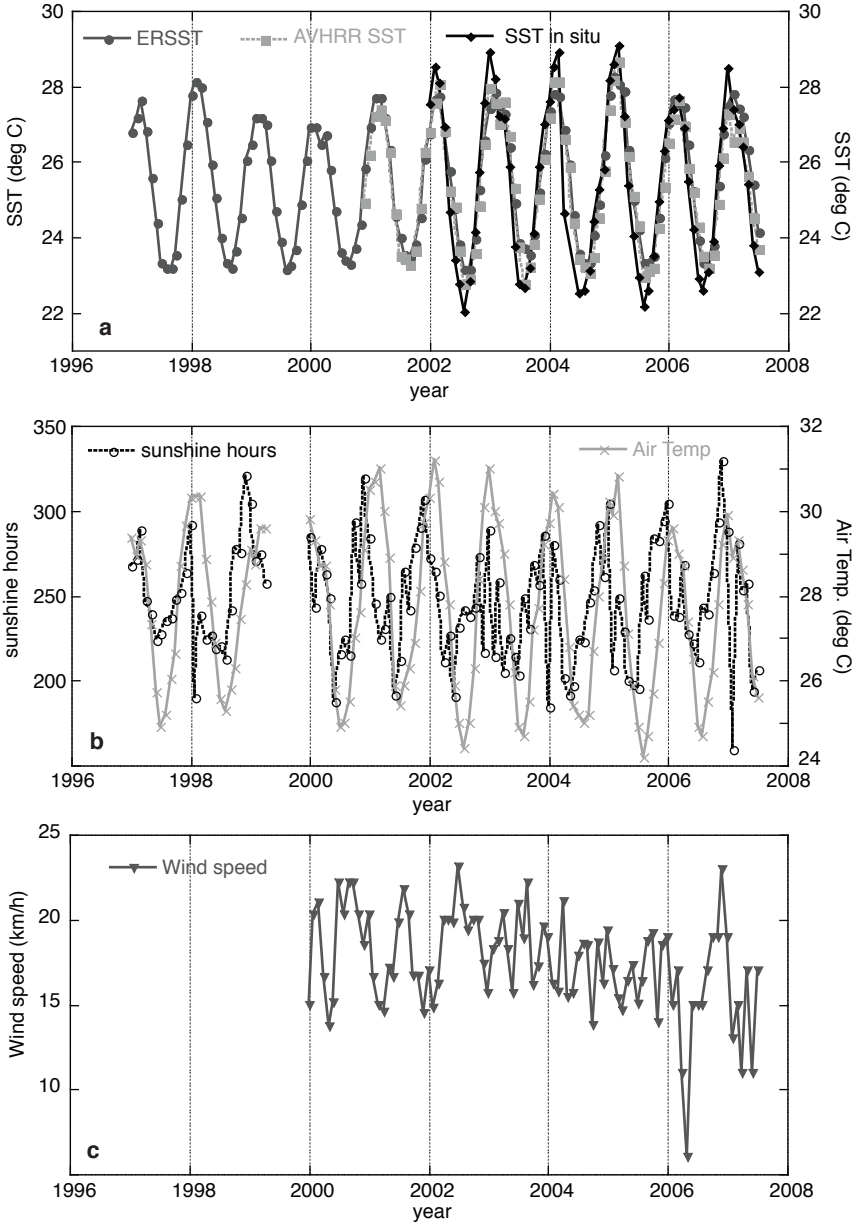

Figure 2

994

995 Figure 2

Biogeosciences Discuss., doi:10.5194/bg-2016-69, 2016
Manuscript under review for journal Biogeosciences
Published: 3 March 2016

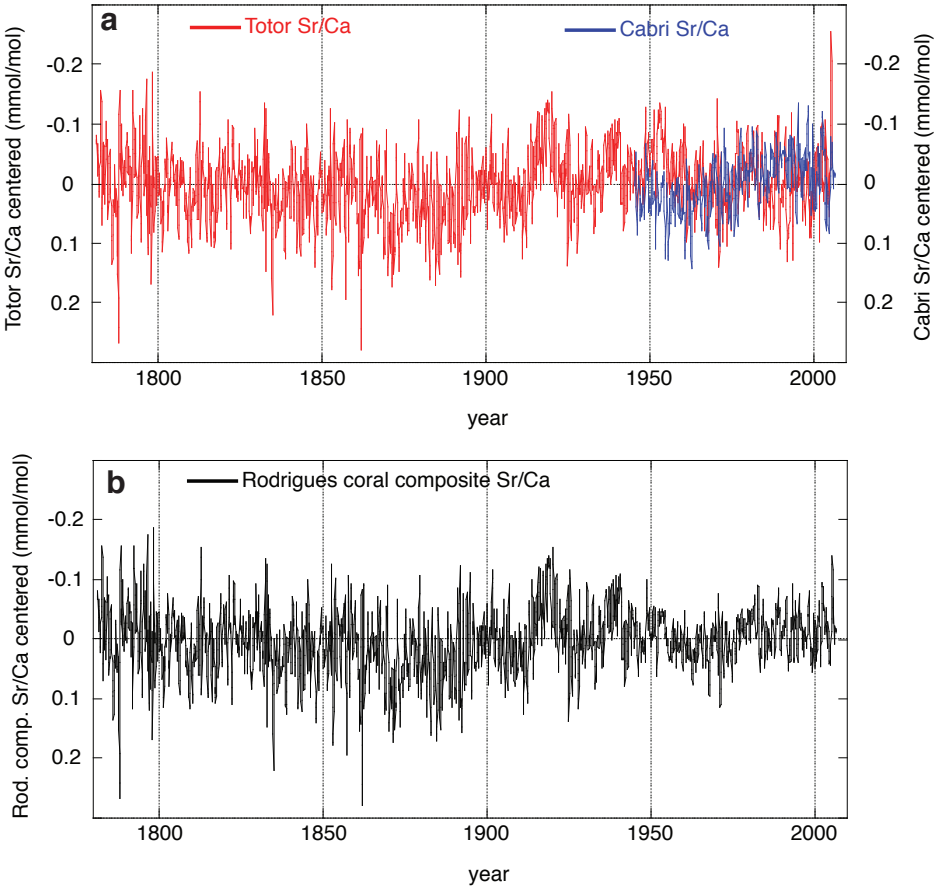

Figure 3

Biogeosciences Discuss., doi:10.5194/bg-2016-69, 2016
Manuscript under review for journal Biogeosciences
Published: 3 March 2016

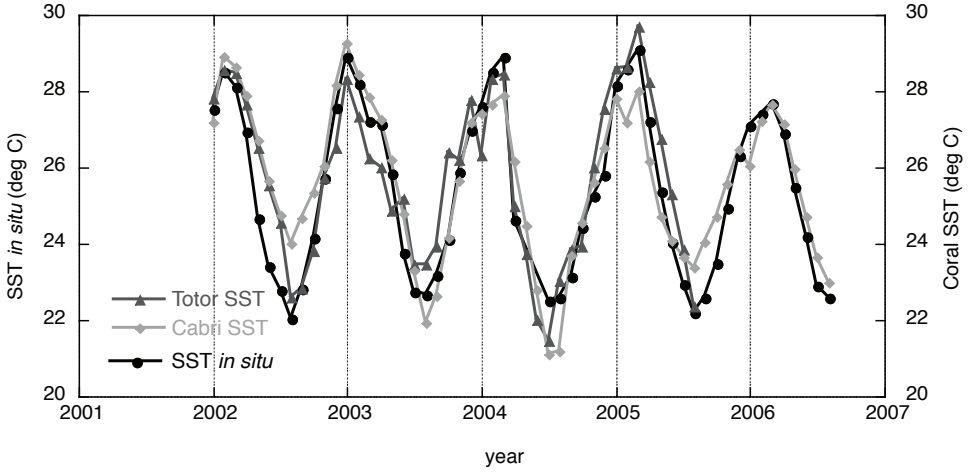

1005

1006 Figure 4

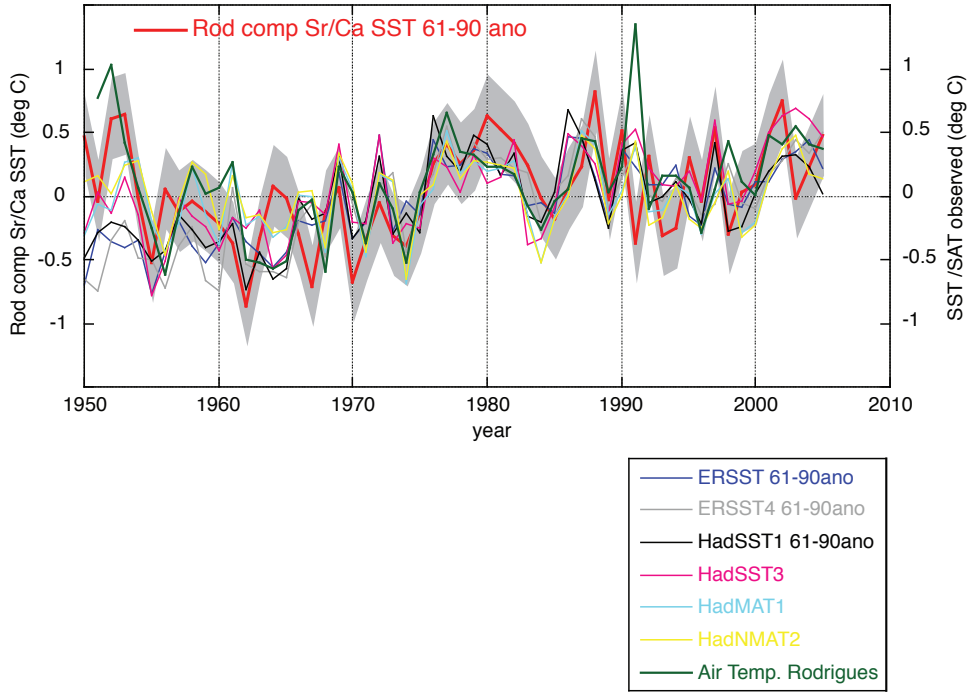

1007

1008 Figure 5

Biogeosciences Discuss., doi:10.5194/bg-2016-69, 2016
Manuscript under review for journal Biogeosciences
Published: 3 March 2016

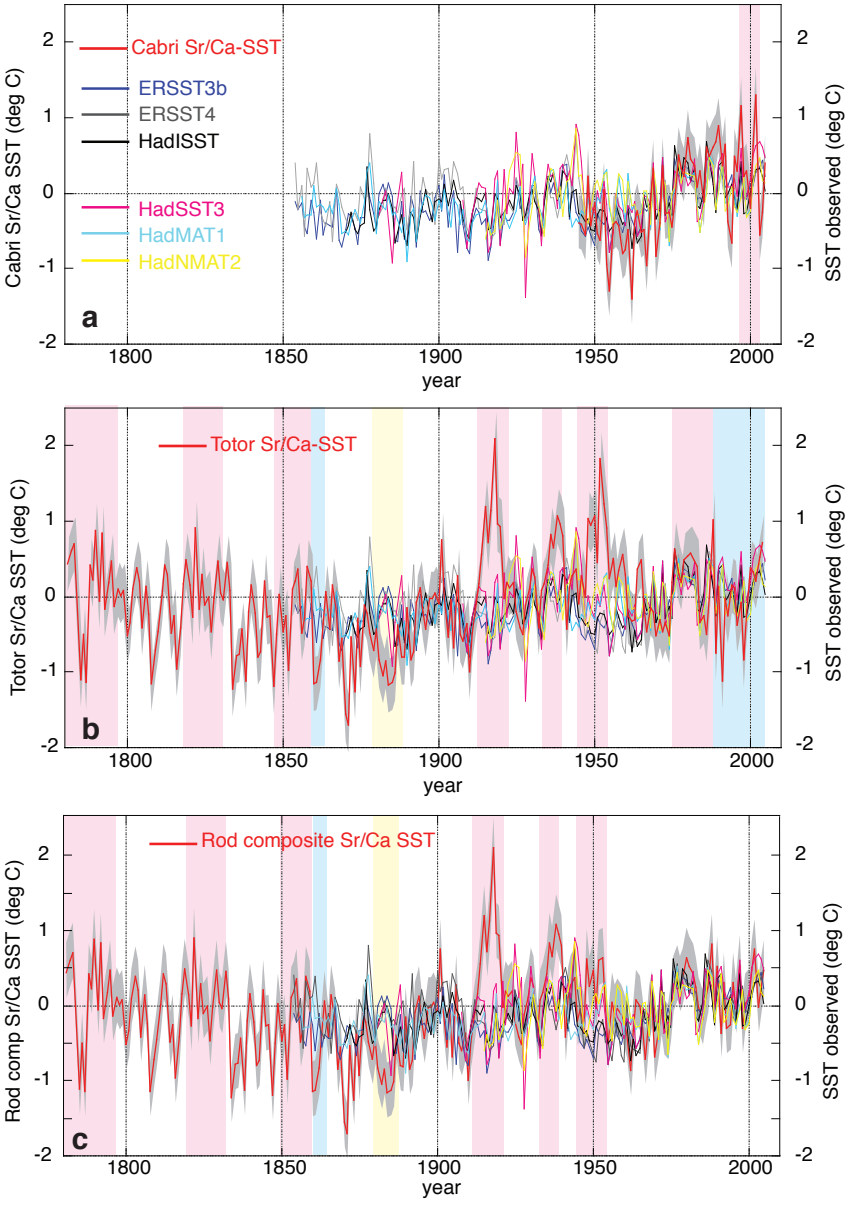

1009

1010 Figure 6

Biogeosciences Discuss., doi:10.5194/bg-2016-69, 2016
Manuscript under review for journal Biogeosciences
Published: 3 March 2016

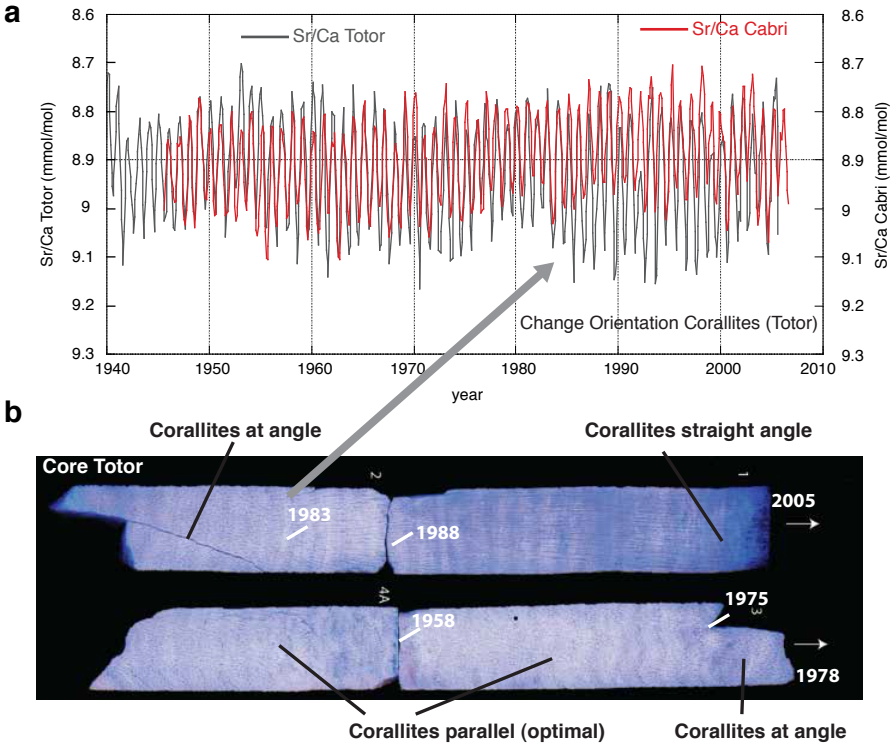

1011

1012 Figure 7

1013

Biogeosciences Discuss., doi:10.5194/bg-2016-69, 2016
Manuscript under review for journal Biogeosciences
Published: 3 March 2016

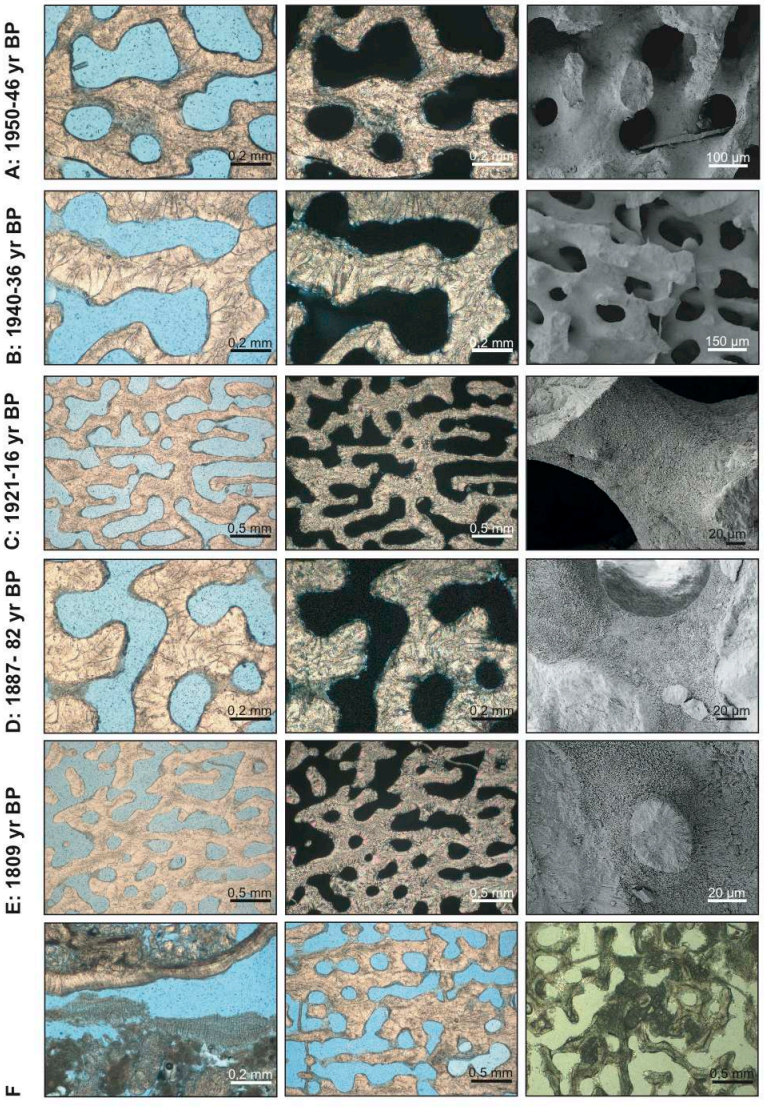

Fig. 8

1014

1015 Figure 8

Biogeosciences Discuss., doi:10.5194/bg-2016-69, 2016
Manuscript under review for journal Biogeosciences
Published: 3 March 2016

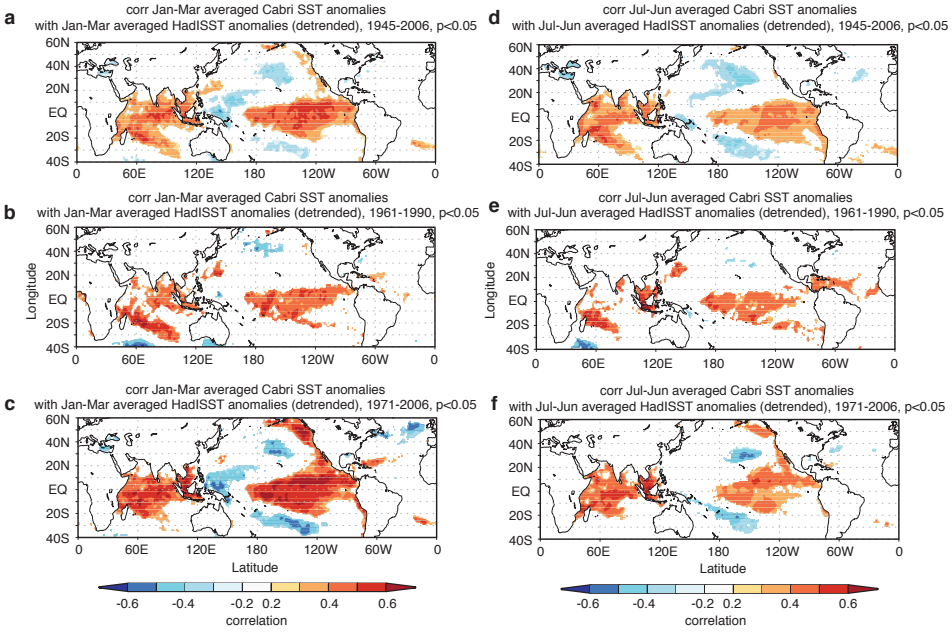

1016

1017 Figure 9

1018

Biogeosciences Discuss., doi:10.5194/bg-2016-69, 2016
Manuscript under review for journal Biogeosciences
Published: 3 March 2016

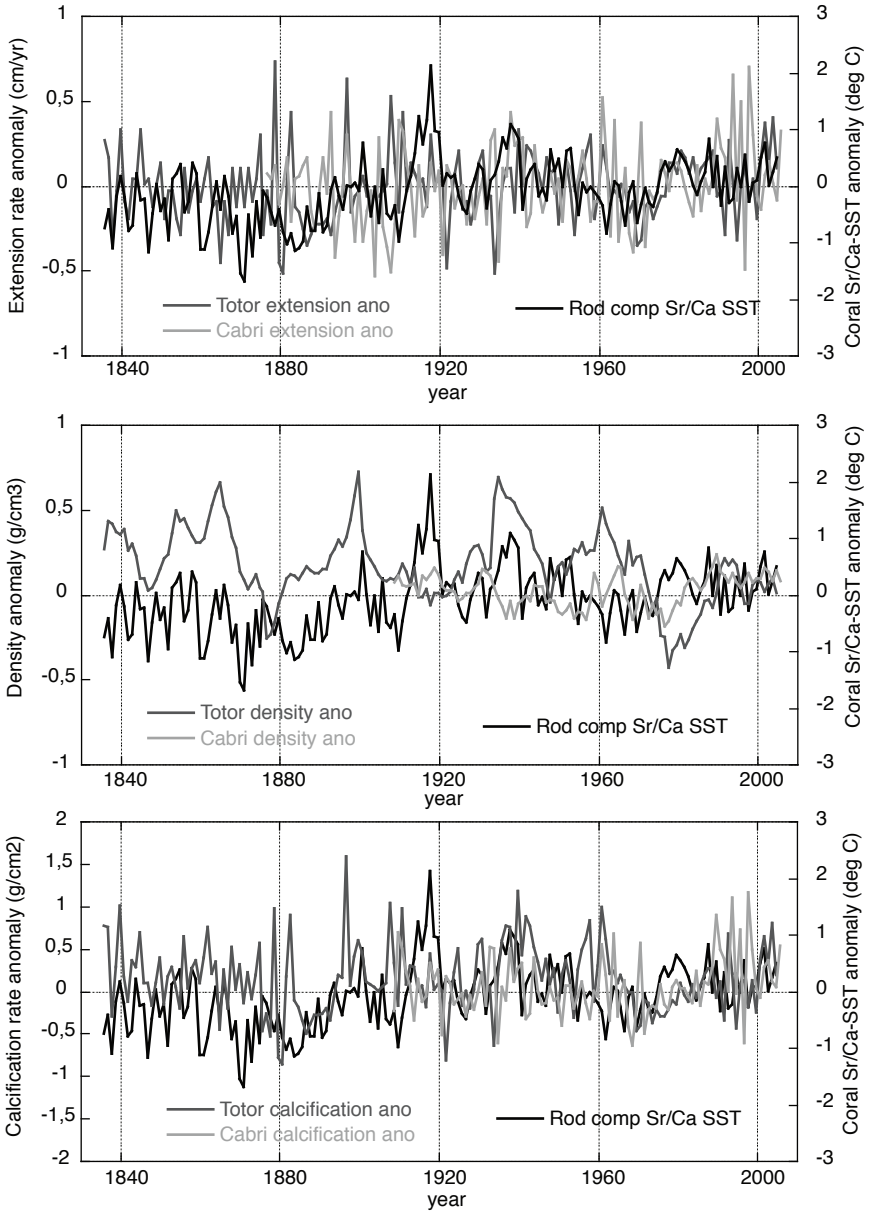

1019

1020 Figure A1

Biogeosciences Discuss., doi:10.5194/bg-2016-69, 2016
Manuscript under review for journal Biogeosciences
Published: 3 March 2016

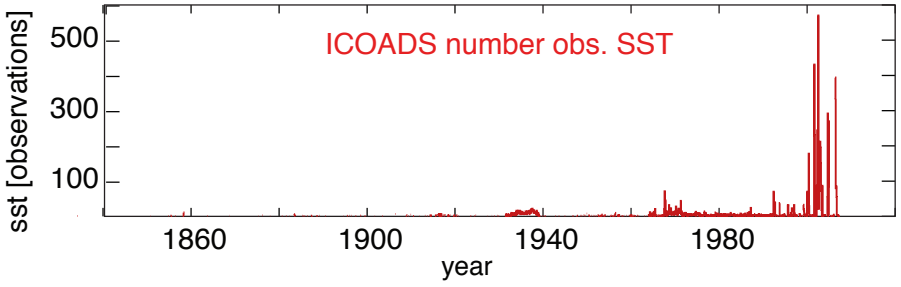

1021

1022 Figure A2

1023

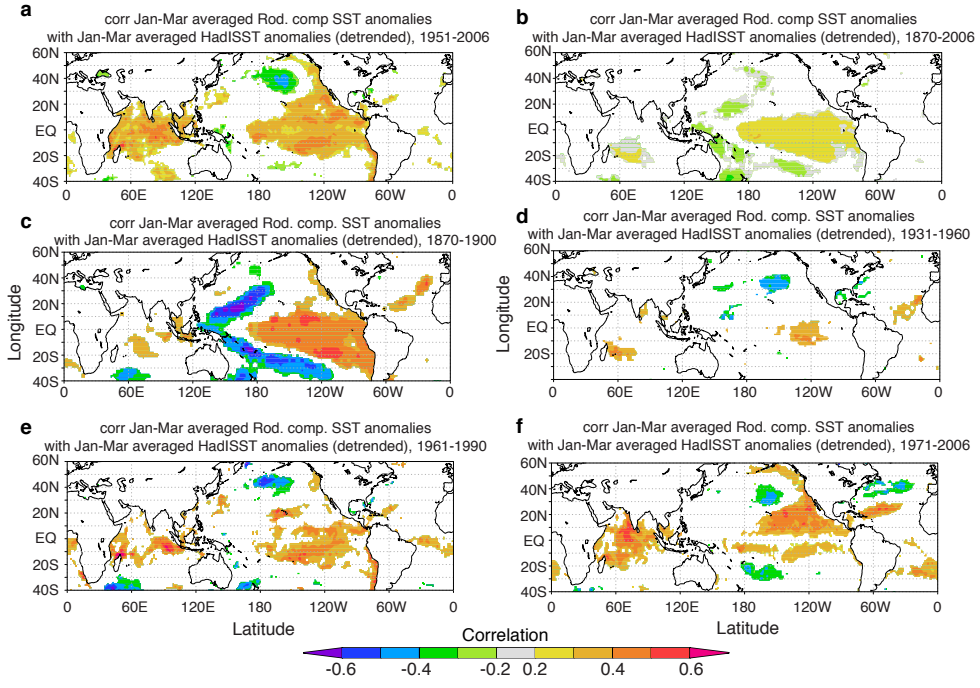

1024

1025 Figure A3

1026

Biogeosciences Discuss., doi:10.5194/bg-2016-69, 2016
Manuscript under review for journal Biogeosciences
Published: 3 March 2016

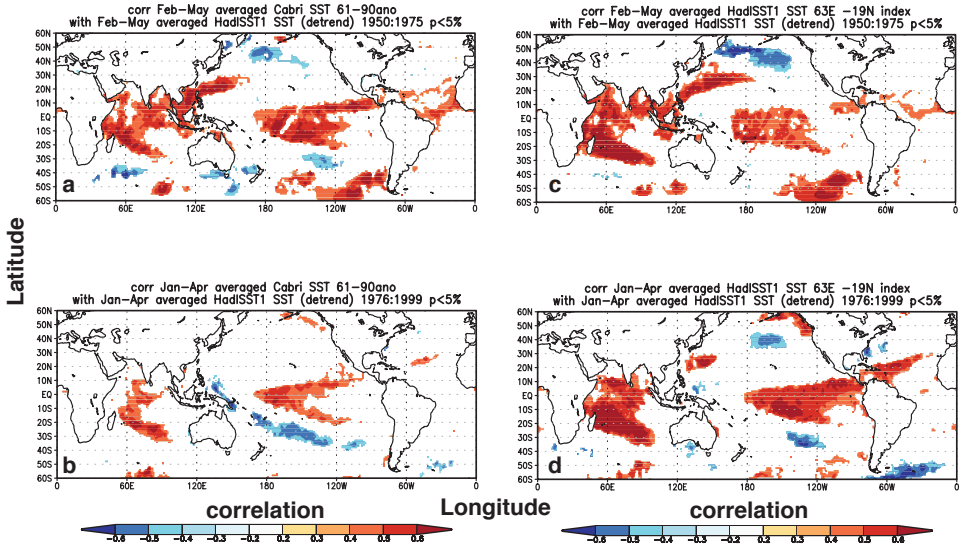

1027

1028 Figure A4

1029

Biogeosciences Discuss., doi:10.5194/bg-2016-69, 2016
Manuscript under review for journal Biogeosciences
Published: 3 March 2016

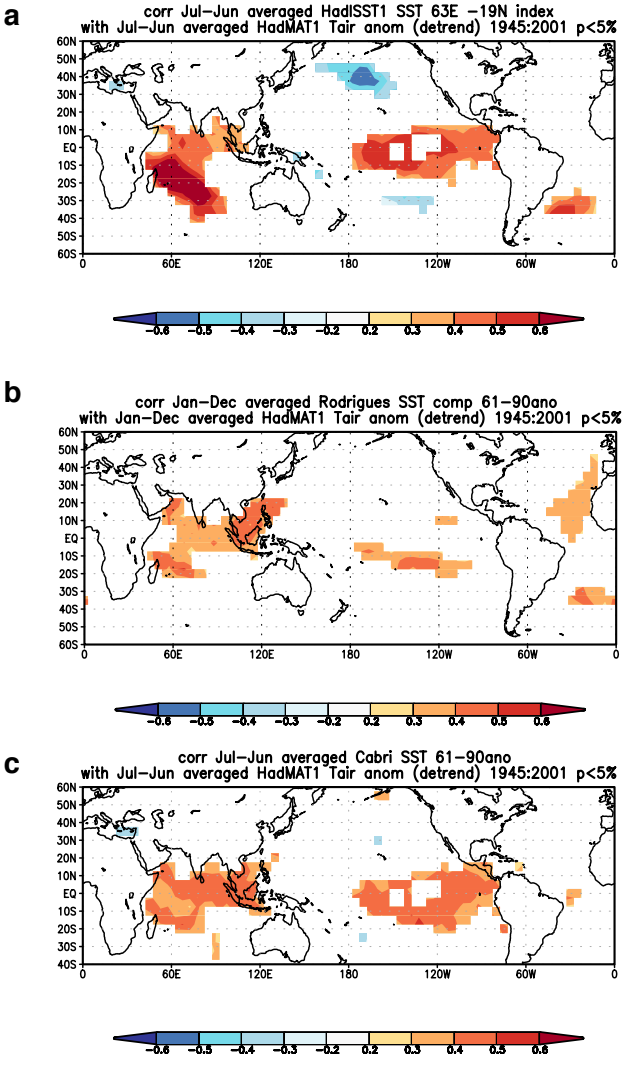

1030

1031 Figure A5

1032

Biogeosciences Discuss., doi:10.5194/bg-2016-69, 2016
Manuscript under review for journal Biogeosciences
Published: 3 March 2016

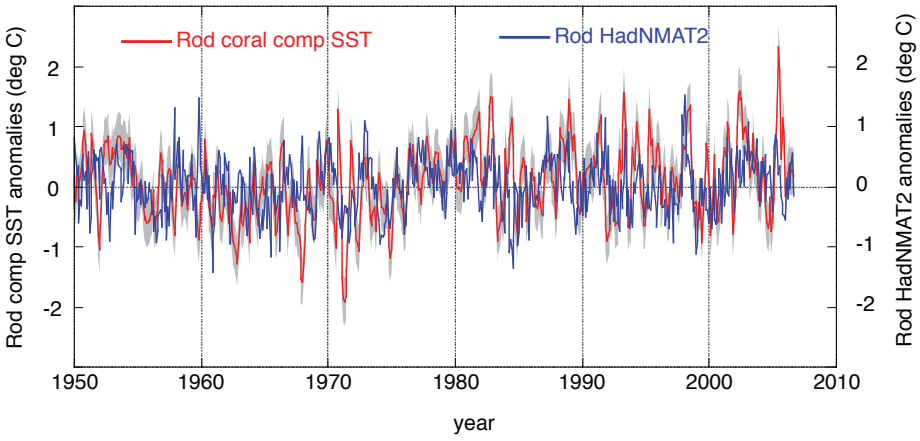

1033

1034 Figure A6

1035

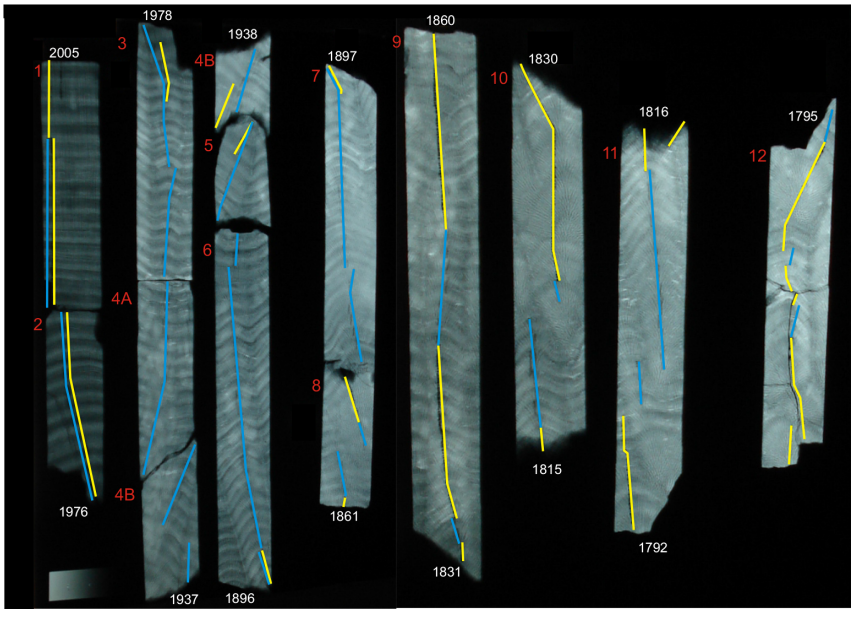

1036

1037 Figure A7

1038

Biogeosciences Discuss., doi:10.5194/bg-2016-69, 2016
Manuscript under review for journal Biogeosciences
Published: 3 March 2016

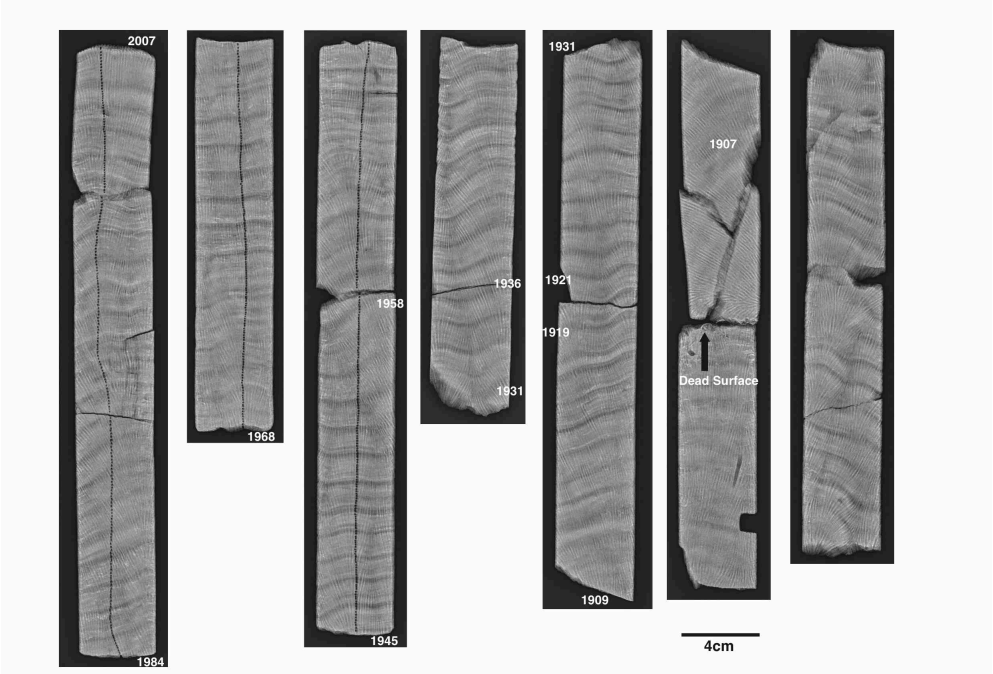

Figure A8

Biogeosciences Discuss., doi:10.5194/bg-2016-69, 2016
Manuscript under review for journal Biogeosciences
Published: 3 March 2016

	SST *in situ* 2002-2006	**AVHRR SST 2002-2006**	**ERSST 2002-2006**	**Air Temp. 2002-2006**
Mean annual	25.49 (0.24)	25.4 (0.11)	25.57 (0.3)	27.49 (0.31)
Maximum	28.6 (0.5)	28.65 (0.44)	28.29 (0.4)	31.2 (0.62)
Minimum	22.4 (0.27)	22.75 (0.21)	23.15 (0.13)	24.2 (0.44)
Seasonal Range	6.22 (0.68)	5.9 (0.58)	5.14 (0.39)	7.0 (0.79)
STDV	2.14	1.78	1.69	2.07

Table A1 – Statistics of various sea surface temperature (SST) products and air temperature for Rodrigues with 1σ standard deviations in brackets for the period 2002 to 2006 (period with *in situ* SST data). STDV = 1σ standard deviation over all years. All units in °C.

Biogeosciences Discuss., doi:10.5194/bg-2016-69, 2016
Manuscript under review for journal Biogeosciences
Published: 3 March 2016

(a) Max-Min	Regression equation	r^2	p
Totor	Sr/Ca = -0.0439(±0.004)*SST + 10.032(±0.10)	0.97	<0.001
Cabri	Sr/Ca = -0.0384(±0.005)*SST + 9.861(±0.12)	0.89	<0.001
(b) Max-Min			
Totor	Sr/Ca = -0.0638(±0.004)*SST + 10.566(±0.09)	0.95	<0.001
Cabri	Sr/Ca = -0.0507(±0.004)*SST + 10.179(±0.10)	0.90	<0.001
(c) Max-Min			
Totor	Sr/Ca = -0.0531(±0.004)*SST + 10.271(±0.11)	0.96	<0.001
Cabri	Sr/Ca = -0.0441(±0.005)*SST + 10.012(±0.13)	0.88	<0.001
(d) Monthly			
Totor	Sr/Ca = -0.0522(±0.003)*SST + 10.272(±0.08)	0.79	<0.001
Cabri	Sr/Ca = -0.0419(±0.003)*SST + 9.95(±0.07)	0.87	<0.001

Table A2 - Linear regression of coral Sr/Ca with a) *in situ* SST 2002-2005/6, b) ERSSTv.3 1997-2005/6, c) AVHRR SST NOAA Coral Reef watch data 2000-2005/6 and d) monthly Sr/Ca with AVHRR SST for the period 1982 to 2005.